

Photometric Properties of Kiso Ultraviolet-Excess Galaxies in the Lynx-Ursa Major Region⁰

Tsutomu T. Takeuchi^{1,2}, Akihiko Tomita³, Kouichiro Nakanishi¹, Takako T. Ishii^{1,4},
Ikuru Iwata⁵, and Mamoru Saitō¹

¹ Department of Astronomy, Faculty of Science, Kyoto University,
Sakyo-ku, Kyoto 606-8502, JAPAN

² Research Fellow of the Japan Society for the Promotion of Science

³ Department of Earth and Astronomical Sciences, Faculty of Education,
Wakayama University, Wakayama 640-8510, JAPAN

⁴ Kwasan and Hida Observatories, Kyoto University,
Yamashina-ku, Kyoto 607-8471, JAPAN

⁵ Toyama Astronomical Observatory, Toyama Science Museum,
49-4 San-no-kuma, Toyama City, Toyama 930-0155, JAPAN

Electronic mail: takeuchi@kusastro.kyoto-u.ac.jp

Received 1998 Aug. 25th; accepted _____

⁰Based on observations made at Kiso Observatory, which is operated by Institute of Astronomy, Faculty of Science, University of Tokyo, Japan.

ABSTRACT

We have performed a systematic study of several regions in the sky where the number of galaxies exhibiting star formation (SF) activity is greater than average. We used Kiso ultraviolet-excess galaxies (KUGs) as our SF-enhanced sample. By statistically comparing the KUG and non-KUG distributions, we discovered four KUG-rich regions with a size of $\sim 10^\circ \times 10^\circ$. One of these regions corresponds spatially to a filament of length $\sim 60 h^{-1}$ Mpc in the Lynx-Ursa Major region ($\alpha \sim 9^{\text{h}} - 10^{\text{h}}$, $\delta \sim 42^\circ - 48^\circ$). We call this “the Lynx-Ursa Major (LUM) filament”. We obtained $V(RI)_C$ surface photometry of 11 of the KUGs in the LUM filament and used these to investigate the integrated colors, distribution of SF regions, morphologies, and local environments. We found that these KUGs consist of distorted spiral galaxies and compact galaxies with blue colors. Their star formation occurs in the entire disk, and is not confined to just the central regions. The colors of the SF regions imply that active star formation in the spiral galaxies occurred 10^{7-8} yr ago, while that of the compact objects occurred 10^{6-7} yr ago. Though the photometric characteristics of these KUGs are similar to those of interacting galaxies or mergers, most of these KUGs do not show direct evidence of merger processes.

Subject headings: galaxies: KUG — galaxies: photometry — galaxies: starburst
— galaxies: statistics

1. INTRODUCTION

Kiso Ultraviolet-Excess Galaxies (hereafter KUGs) are a blue galaxy sample selected from photographic *UGR* three-color images taken by the Kiso Observatory 105-cm Schmidt telescope (Takase & Miyauchi-Isobe 1993, and references therein, hereafter TM93). The survey selected galaxies if they had a greater UV excess than A-type stars seen on the same plates. The KUG survey has been carried out mainly on the northern celestial hemisphere over $\sim 5800 \text{ deg}^2$, and contains roughly 8200 objects. The depth of the survey is $17 \sim 18.5$ mag in photographic magnitude. A second KUG survey is in progress. A general description of the survey method and the statistical properties of KUG objects is given in Takase (1980).

A galaxy that has experienced a star formation (SF) episode less than $\sim 10^{8-9}$ yr (sub-Gyr) ago contains an elevated number of A stars and so can be identified by a bluer than average color. The so-called Butcher–Oemler galaxies are mostly in this category (Dressler & Gunn 1983). Photometric (Maehara et al. 1988), spectroscopic (Maehara et al. 1987, 1988; Augarde et al. 1994; Comte et al. 1994), and radio (Maehara et al. 1985, 1988) observations have revealed that KUGs as a class exhibit star formation. Thus, the KUG survey is a good sample of galaxies to use in examining objects that have experienced periods of star formation within the recent sub-Gyr in the Local Universe. Tomita et al. (1997)(TTUS97) have quantified the general characteristics of a large number of KUGs using optical color, morphology, and FIR data. Here we briefly summarize their results.

1. The KUG selection was originally based on a plate search, and the classification of galaxies into blue and non-blue ones proved to work well even in terms of the total color systems, but the boundary color is slightly redder than that of A-stars; that is, 22 % of the KUGs have the non-KUG colors, and the boundary color separating KUGs and non-KUGs is $(U - V)_T = 0.1 \text{ mag}$.

2. KUGs are preferentially Sb- or later-type spiral galaxies. The KUG fraction changes linearly along the Hubble sequence: it is less than 10 % for E/S0 and more than 50 % for Sd/Sm.
3. KUGs are biased toward less luminous galaxies. At around the knee of the luminosity function (LF) where B -luminosity $L_B \sim 10^{10} L_\odot$, most of the KUGs are spiral galaxies. In the fainter regime of $L_B < 10^{9.3} L_\odot$, the dwarf population dominates.
4. The fraction of the blue population in a survey depends on the depth of the survey. If the survey is volume-limited and deep enough to pick up the bulk of the dwarf population, its fraction would be higher.

The distribution of KUGs is inhomogeneous, not only when compared with a uniform distribution but also in comparison with the ambient galaxy distribution. Consequently there are some “KUG-rich regions”. This inhomogeneity may be related to environmental effects. Some studies show that a dense environment activates star formation (e.g. Maia et al. 1994; Pastoriza et al. 1994). On the other hand, recent observational studies (e.g. Zabludoff et al. 1996(Z96)) suggest that a low-density environment can enhance star formation. Therefore, the question is unsettled.

In this study we statistically analyzed the fraction of KUGs in the whole galaxy population and discovered four KUG-rich regions. Among them was a region which lies in the constellations of Lynx and Ursa Major ($\alpha \sim 9^{\text{h}} - 10^{\text{h}}$, $\delta \sim 42^\circ - 48^\circ$). In this region, there is a galaxy filament with a length of $\sim 60h^{-1}$ Mpc (We use $H_0 = 100h \text{ km s}^{-1} \text{ Mpc}^{-1}$ as the Hubble parameter throughout this paper). We call this structure the Lynx-Ursa Major (hereafter LUM) filament. We obtained $V(RI)_C$ surface photometry of eleven KUGs in this region in order to make a quantitative analyses of the star formation properties and effects of local environment on star formation.

This paper is organized as follows: Section 2 describes our statistical survey methods and the KUG-rich regions found. Sample selection, observation, and data reduction of the $V(RI)_C$ photometry of the eleven KUGs in LUM filament are discussed in section 3. Section 4 presents the results of our photometry. Discussion based on the photometry is made in section 5. Finally in section 6, we present a summary of our results.

2. SURVEY

2.1. KUG-rich Regions

First we searched for regions in which the total galaxy population contains a large fraction of KUGs. A single Kiso Schmidt plate has a field of view of $6^\circ \times 6^\circ$. The previously noted variation in survey depth is caused by differences in plate quality. To avoid a bias caused by the variation of the photographic-plate depths, we required that our sample galaxies also be included in the magnitude-limited portion of the *Catalogue of Galaxies and of Clusters of Galaxies* (Zwicky et al. 1961 – 1968, CGCG). This limited our sample to objects with $m_{pg} \lesssim 15.7$ mag. (corresponding to $m_{BT} \lesssim 15.2$ mag, Kirshner et al. 1978) at $\delta > -5^\circ$. Although the faint limit of the CGCG has some uncertainties (e.g. Takamiya et al. 1995), they do not affect our analysis. Hereafter we use the term KUG for galaxies listed in both the CGCG and KUG catalogs.

The KUG population fraction, f_{KUG} , was defined as $f_{KUG} = k/n$ where $n =$ [the total number of CGCG galaxies on a plate] and $k =$ [the number of KUGs on the same plate]. We first formed this statistic for the individual $6^\circ \times 6^\circ$ photographic plates. Using only this number, we found some tentative “KUG-rich” regions. We were still concerned, however, that these could be false effects caused by the differing depth of each photographic plate. To check on this we recalculated f_{KUG} for the same sized areas in an offset “tessellation” that

was independent of the location of the original Kiso fields. Both methods yielded almost the same result, implying that the effects of the plate-quality difference was effectively suppressed by using the CGCG subsample. We also formed the f_{KUG} statistic for areas with sizes ranging between $3^\circ \times 3^\circ$ and $10^\circ \times 10^\circ$, again with no significant change in results. Figure 1 shows the distribution of f_{KUG} versus n . Each symbol represents f_{KUG} of a $6^\circ \times 6^\circ$ -area from the offset tessellation.

The next step was to determine the statistical significance of the KUG-rich regions. As shown in Fig. 1, the mean KUG fraction has a value of $\sim 27.7\%$ which is essentially independent of n . We therefore assumed that $p = 0.277$ represents the mean KUG fraction. The probability density of k with respect to n , $P(n, k)$, follows a binomial distribution given by

$$P(n, k) = \frac{n!}{(n-k)!k!} p^k (1-p)^{n-k} \quad k = 1, \dots, n, \quad (1)$$

The standard deviation, σ , is

$$\sigma = \sqrt{np(1-p)} \quad . \quad (2)$$

The probability $P(n, \xi)$ that f_{KUG} has the value $f_{\text{KUG}} = \xi$ in a population of n CGCG galaxies is

$$P(n, \xi) = \frac{n(n!)}{(n-n\xi)!(n\xi)!} p^{n\xi} (1-p)^{n(1-\xi)} \quad 0 \leq \xi \leq 1. \quad (3)$$

Equations (2) and (3) give a standard deviation for ξ , $\sigma_\xi(n)$, of

$$\sigma_\xi(n) = \sqrt{\frac{p(1-p)}{n}} \quad . \quad (4)$$

The smaller n is, the larger $\sigma_\xi(n)$ becomes. This is well expressed in Fig. 1 which shows confidence limits of 99.9%, 99.99%, and 99.999% as long-dashed, dotted, and dashed lines. We define the KUG-rich regions as those in which f_{KUG} is greater than or equal to

the 99.99% confidence limit. The filled symbols in Fig. 1 represent the KUG-rich regions. Eight filled symbols are plotted in Fig. 1, but B overlaps one of the Ds, and C overlaps one of the Es making the number of filled symbols appear as six. Circles with the same labels are regions adjacent to each other on the sky. The large extent of the regions and the high confidence limit both show that these regions are not mere products of chance.

An all-sky map containing the KUG-rich regions we discovered is shown in Fig. 2. In this figure the small dots represent the distribution of CGCG galaxies in KUG-survey regions, and the black hatches depict the KUG-rich regions. Their labels (A, B, C, D, and E) correspond to the same labels in Fig. 1. KUG-rich region E contains the galaxy cluster Zwicky 1615.8+3505. Unfortunately, this contains KUG area A0432 (center position: $16^{\text{h}}20^{\text{m}}, +35^{\circ}$), which has been reported to contain a sizable fraction of non-blue galaxies that should not have been in the Kiso survey (Miyauchi-Isobe, Takase, & Maehara 1997). The cluster itself has other interesting aspects, the details of which will be presented elsewhere (Tomita et al. 1998). Other four regions have no virialized galaxy structures, i.e., they are in the “field”. Details on region A are presented in section 2.2. Region B seems to be a part of a filamentary structures of galaxies in proximity to Canes Venatici void. Region C may also belong to a filament surrounding the Gemini void, and region D may associate with a filament between the Leo and Coma voids that is connected to the Coma cluster (Fairall 1998). We summarize the parameters of these KUG-rich regions in Table 1. Column 1 gives the labels of KUG-rich regions presented in Fig. 1 and Fig. 2. Their approximate positions are given in columns 2 and 3, and corresponding KUG field numbers are shown in column 4. Since the offset tessellation defines a grid centered different from the original Kiso survey field blocks, the black-hatched regions in Fig. 2 and the Kiso fields given in column 4 of Table 1 are at slightly different positions.

2.2. The Lynx-Ursa Major (LUM) Filament

Around region A, we found a filament structure of galaxies in the CfA survey (e.g. de Lapparent, Geller, & Huchra 1986). We name it “the Lynx-Ursa Major (LUM) filament” after the constellation it lies in. This is an elongated and winding structure extending along the line of sight between $cz \sim 2000 \text{ km s}^{-1}$ and 8000 km s^{-1} ($\sim 60h^{-1} \text{ Mpc}$), at $\alpha \sim 9^{\text{h}} - 10^{\text{h}}$, $\delta \sim 42^\circ - 48^\circ$. The far end of the filament connects to the Great Wall (Geller & Huchra 1989). We note that, although “the Lynx-Ursa Major supercluster” named by Giovanelli & Haynes (1982) and the LUM filament are connected, these are actually distinct structures, and the former is much larger. Han et al. (1995) studied the orientation of the spin vectors of galaxies belonging to a filamentary structure in this area. They named it “the Ursa Major filament”. Their filament is part of the left leg of the “CfA homunculus”, and differs from our LUM filament. As mentioned above, region D is associated with Han et al.’s filament.

We summarize the parameters of the LUM filament in Table 2.

3. OBSERVATION AND DATA REDUCTION

3.1. The Sample

We obtained surface photometry of the KUGs in the LUM filament that met the following selection criteria: (1) an angular diameter $\gtrsim 0.6$, (2) a small inclination (axial ratio $\lesssim 2$). The first criterion was to ensure the sample galaxies were large enough to allow the identification and analysis of their star-forming regions. The second criterion was to minimize the effect of internal extinction on the objects, the correction of which is uncertain (Buta & Williams 1995, hereafter BW95). Eleven objects met these criteria. We compile their names, positions, and basic properties in Table 3. Column 1 gives the serial

number of the objects, and columns 2 and 3 give their KUG and CGCG names respectively. Columns 4 and 5 give their positions (B1950.0 equinox) extracted from NED. Columns 6 and 7 give their recession velocity and B_T^0 Magnitudes, both from *Third Reference Catalogue of Bright Galaxies* (de Vaucouleurs et al. 1991, hereafter RC3). The recession velocities are galactocentric. Column 8 gives the absolute B -magnitude of the objects calculated from cz and B_T^0 . All of the samples are *IRAS* point sources.

Next we examine whether our selected sample is fair or not. The LUM filament lies at $cz \sim 2000 \text{ km s}^{-1}$ to 8000 km s^{-1} . Among the 11 sample KUGs, No. 1 is the nearest, Nos. 2, 3, 6, 7, 8, and 9 are located in the nearer half of the filament, Nos. 5 and 10 in the further half, and Nos. 4 and 11 at the further end. Therefore our sample is not strongly correlated with redshift in the manner of the KUG and CGCG (see Fig.7 of TTUS97). Next we check the galaxy luminosities. The LF of the KUGs show Schechter-like behavior (Schechter 1976), with a knee at $L_B \sim 10^{10} L_\odot$, corresponding to $M_B \sim -19.45 \text{ mag}$ (TTUS97). The brightest object is No. 11 ($M_B = -20.71 \text{ mag}$) and the faintest is No. 9 ($M_B = -18.20 \text{ mag}$). The others distribute rather uniformly between the two. Our sample consists of slightly bright KUGs, but as a whole, it is not strongly biased toward brighter luminosities. We note that there are no AGNs in the sample.

3.2. $V(RI)_C$ Surface Photometry and Data Reduction

We obtained $V(RI)_C$ surface photometry using the 105-cm Schmidt telescope at the Kiso Observatory (hereafter Kiso). The nights were photometric and had seeing conditions of typically a few arcseconds. The observation log is given in Table 4. Column 1 shows the names of the sample KUGs. The observed date is presented in column 2. Column 3 gives the ID numbers of the obtained original CCD image frames at Kiso.

The optical system at the prime focus has a focal ratio of $F/3.1$. We mounted at the prime focus a single-chip CCD camera which uses a TI Japan TC215 frontside-illuminated 1000×1018 chip. One pixel size corresponded to $0''.752$, giving a total field of about $12'.5 \times 12'.7$. Nonlinearity was $< 0.5\%$ at < 25000 counts, which is too small to give rise to any significant photometric error. We used broadband Johnson V , Cousins R_C , and I_C filters. The Kiso V -, R_C -, and I_C -band response functions are in good agreement with the standard filter transmissions so we did not need any color corrections. The exposure time for all objects and filters was 900 sec.

The basic data reduction consisted of a bias subtraction, flatfielding, and cosmic-ray elimination, using IRAF¹. Sky subtraction was accomplished via a polynomial-surface fit to the sky regions using SPIRAL (Hamabe & Ichikawa 1992). We made various tests to estimate the uncertainty of the sky subtraction, which turned out to be $\lesssim 1\%$.

Flux calibration was done by observing the equatorial photometric standard stars of Landolt (1992) throughout the night. The differences of the standard magnitudes from the original values of Cousins for our V -, R -, and I -bands are small enough (Menziés et al. 1991), to preclude making any corrections. We obtained integrated magnitudes for each object from the asymptotic limit of a circular-aperture curve of growth after any stars were removed from the galaxy image. We used the template curve of growth provided by Kodaira, Okamura, & Ichikawa (1990) for testing the convergent value of the curve of growth. The reliability of this method is examined in Tomita et al. (1998). The total error induced by all procedures is typically ~ 0.03 mag.

¹IRAF is distributed by National Optical Astronomy Observatories (NOAO), which is operated by the Association of Universities for Research in Astronomy, Inc., under contract to the National Science Foundation.

In order to better estimate the colors of the objects, we corrected for differences caused by variations in the seeing size and position between the images taken in different bandpasses. We used IRAF and SPIRAL for this procedure. For the detailed color analysis we used IDL (Interactive Data Language).

4. RESULTS

4.1. Total Magnitudes by Growth-curve Fitting

We show the results of the photometry in Table 5. Column 1 gives the name of the galaxy. Columns 2, 3, and 4 give the apparent integrated V -, R_C -, and I_C -magnitudes respectively. No correction for internal or external extinction has been applied for the *apparent* magnitudes. Columns 5, 6, and 7 give the derived total absolute magnitudes after correction for Galactic extinction. The Galactic extinction value at Lynx – Ursa Major, derived from the maps of Burstein & Heiles (1982), is $E(B - V) \sim 0.03$. This corresponds to $A_V \sim 0.09$ mag, $A_R \sim 0.07$ mag, and $A_I \sim 0.04$ mag when we apply $R_V = A_V/E(B - V) = 3.1$, using the extinction curve of Cardelli, Clayton, & Mathis (1989). Absolute magnitudes are dereddened by these values. We did not apply any correction for inclination. No attempt has been made to apply K -correction because of the closeness of our sample.

These are the first photometric measurements for all but one of these objects, KUG0953+466. This object is also Mrk 129 (Markarian et al. 1989), and has Johnson V - and R - band photometry from Huchra (1977)(H77). Using $24''$ -aperture photometry, the same aperture size as H77, we measured the V - and R_C -magnitudes for comparison. Then we converted his R -magnitude to R_C . (We also use this conversion in section 5.2, where a detailed discussion of the conversion formula will be given.) Table 6 shows our results and

shows that our measurements are identical with the values from H77, to within the errors.

4.2. Contour Maps

Figure 3 shows contour maps in the V - and I_C -bands of all 11 objects in our sample. They are shown from top to bottom in increasing order of right ascension, α . The contour interval is 0.5 magnitudes. In this figure, north is above, and east is to the right. The FOV is $2'5 \times 2'5$. A distance scale bar of $10 h^{-1}$ kpc is presented in the upper-left of each galaxy image. We comment on the morphological feature of each galaxy. Unless otherwise noted, the morphological index is the T -type from the RC3.

KUG 0908+451 (NGC 2766, IRAS F09089+4509) The morphological index is $T = 5$. This galaxy is quite knotty, with a large number of HII regions. This object has a globally distorted appearance, and well-developed arms. The eastern arm is extremely blue. There are no companions in the FOV of the Kiso CCD (corresponding to $\sim 100h^{-1}$ kpc \times $100h^{-1}$ kpc).

KUG 0908+468 (Mrk102, IRAS F09082+4650) A morphological index is not given in the RC3, and cannot be accurately estimated. This is a featureless, spheroidal galaxy, with a slightly boxy isophote. It is isolated in $\sim 160h^{-1}$ kpc \times $160h^{-1}$ kpc.

KUG 0911+471 (UGC 4870, IRAS F09115+4706) A morphological index is not given in the RC3. We estimate a value of $T \sim 5$. The disk is slightly warped. This galaxy has HII-region knots in its peripheral region around the disk which are not well presented in the smoothed contours. There are no galaxy companions in $\sim 160h^{-1}$ kpc \times $160h^{-1}$ kpc.

KUG 0919+474 (Mrk109, IRAS F09190+4727) A morphological index is not given in the RC3, and cannot be accurately estimated. This object has a compact and featureless appearance. It lies in a loose group of galaxies and has some companions.

KUG 0924+448 (UGC 5045, IRAS F09249+4452) The morphological index is $T = 5$. This object is a triple-arm barred galaxy which suffers from global distortion. Its arms are knotty with many HII regions. It is isolated in a field of $\sim 270h^{-1} \text{ kpc} \times 270h^{-1} \text{ kpc}$.

KUG 0944+468 (UGC 5237, IRAS F09441+4650) The morphological index is $T = 6$. The object is asymmetric. The arm in the south is well-developed with large blue knots. It is isolated in a field of $\sim 160h^{-1} \text{ kpc} \times 160h^{-1} \text{ kpc}$.

KUG 0945+443 (NGC 2998, IRAS F09455+4418) The morphological index is $T = 5$. This galaxy has extremely well-developed knotty arms. It lies in a loose group, and there is a faint irregular galaxy lying at $5'$ ($\sim 60h^{-1} \text{ kpc}$) to the east. They do not appear to be bridged, or have any features which imply interaction.

KUG 0947+445A (NGC 3009, IRAS F09470+4431) A morphological index is not given in the RC3. We estimate a value of $T \sim 4$. This galaxy has four-arms, with the one in the north being less developed than the others. The appearance is rather smooth with no prominent HII-regions. It lies in a loose group, and has small companions in almost the same redshifts, but without any tidal features.

KUG 0953+466 (Mrk129, IRAS F09535+4641) A morphological index is not given in the RC3, and cannot be accurately estimated. This object is a featureless, boxy-shaped compact galaxy. It is isolated in $\sim 160h^{-1} \text{ kpc} \times 160h^{-1} \text{ kpc}$.

KUG 1007+461 (NGC 3135, IRAS F10078+4611) A morphological index is not given in the RC3. We estimate a value of $T \sim 5$. Its arms are ill-developed. This galaxy has a companion in the north-east.

KUG 1016+467 (NGC 3191, IRAS F10159+4642) The morphological index $T = 4$. This galaxy suffers from heavy distortion, and has a companion to the west. There is an extremely blue tidal bridge between them suggesting that they are interacting.

4.3. Colors

We give the total integrated $V(RI)_C$ colors of the objects in Table 7. They are corrected only for Galactic extinction.

We then further divided each image into sections and derived colors section-by-section in order to investigate the distribution of SF regions within each galaxy. An SF region that is 2 – 3 kpc diameter (which is typical of such regions) has an angular size of $\sim 7''$ at $cz \sim 9000 \text{ km s}^{-1}$, the distance of the furthest galaxy in our sample. This angular size is much larger than the seeing disk of our images, therefore we can divide the most distant image into $7'' \times 7''$ -sized squares without oversampling. For consistency we scaled the sample resolution applied to our nearer objects with redshift to match the same physical size of 3 kpc. Then, for the regions which have $S/N > 3$, we evaluated the colors. Figure 4 shows the partitioning of each galaxy. Color-color (C-C) diagrams of the sections in each galaxy are presented in Fig. 5. The dominant error of the color estimation comes from the sky fitting. Points labeled “bulge” and “disk” are from those sections of each galaxy respectively. For some representative regions in each galaxy, we have labeled its number from Fig. 4 beside the corresponding point in Fig.5. The three broken lines on the C-C diagrams show starburst evolutionary tracks superimposed on an old stellar population

(Bica, Alloin, & Schmidt 1990, hereafter BAS90). Detailed discussion about these tracks will be given in section 5.2.

5. DISCUSSION

5.1. Total Colors

We compare the total colors of our sample with those of galaxies listed in the RC3. We have taken our values for $(V - R)_T^0$ and $(V - I)_T^0$ From BW95. Their filters are the same as those of Kiso, Johnson V , and Cousins R_C and I_C , so it was not necessary to apply a correction. However, they corrected the galaxy colors for internal extinction and inclination. To compare our results with the data from by BW95, we applied a correction of $A_V \sim 0.15$ for internal extinction.

Fig. 6 plots $(V - R)_T^0$ versus $(V - I)_T^0$ for the KUGs in the LUM filament together with those of a wider range in Hubble type from BW95. Open circles represent the mean color of each morphological type index T ². The errors bar give the standard deviation in each color across the galaxies belonging to each morphological type. Filled squares represent the dereddened colors of our KUGs. The applied reddening correction vector is presented in the top left of the diagram. The typical photometric error of our data is shown in the bottom right. The reddening correction value is set to compare our photometry with that of BW95. The morphological T -index of each KUG is indicated. For the six objects without T in RC3, we use our own classification or label them as “C” for compact morphology if we could not determine a T value. The colors of our sample tend to deviate systematically blueward from the range of the 1σ -strip of the Hubble sequence in $(V - I)_T$. Even though our

²The shown indices are $-5, -4, -3, -2, -1, 0, 1, 2, 3, 4, 5, 6, \{7 \text{ and } 8\}, 9$, and 10 , according to BW95.

sample consists of intermediate/late-type spiral and compact galaxies, they are scattered well outside the distribution of the BW95 sample. This is attributed not only to the blue continuum emission from early-type stars but also to the strong emission lines from star forming regions. The strong $H\alpha$ line makes their $(V - R)$ color redder, which is clearly seen in Fig. 6.

A similar tendency has been reported for other UV-excess galaxy samples. Markarian galaxies are dispersed on a $(U - B)$ - $(B - V)$ diagram wider than field galaxies (H77). Barth, Coziol, & Demers (1995, hereafter BCD95) have mentioned that their Montreal Blue Galaxy (MBG) sample shows a larger dispersion than normal galaxies on the $(B - V)$ - $(V - R)$, and $(B - R)$ - $(V - I)$ planes. The MBG is a blue galaxy sample selected by a similar but more restricted method than the KUG survey (Coziol et al. 1996, and references therein). Larson & Tinsley (1978) pointed out that interacting galaxies show a large scatter on C-C diagrams. Therefore, BCD95 have suggested a link between active star formation in MBG and galaxy-galaxy encounter, since such behavior of interacting galaxies is similar to those of their samples. Our analysis, however, shows that the blue color of KUGs is not necessarily connected to interactions (see section 5.3).

5.2. Distribution of SF Regions

Figure 5 clearly shows that all the spiral KUGs of our sample have bulges redder than their disks, like normal galaxies. This means that the LUM-filament KUGs are not starburst nucleus galaxies (SBNGs), a fact consistent with the KUG morphological types given in the original catalog. This is in contrast to the fact that the most MBGs are SBNGs (Coziol et al. 1996). A detailed discussion on morphology is in section 5.3. The rest of our sample turns out to be compact galaxies. These compact galaxies are not too distant to judge their morphology ($cz \sim 5000 \text{ km s}^{-1}$), and are in reality featureless. Their properties

are similar to those of the so-called blue compact dwarf galaxies (BCDGs), but our compact KUGs have $\log L_B > 9.5$ ($M_B < -18.2$ mag), brighter than BCDGs. This is consistent with the global properties of the whole KUG survey (TTUS97, and references therein).

A comparison of the starburst evolution models with the color distribution in Fig. 5 provides an estimate of the onset of star formation in each object. As previously noted, we used evolution tracks from BAS90, which describe the spectral evolution over 3×10^9 yr of a starburst in low metallicity gas, superimposed on an older stellar population. Their models combine elements from star cluster and galaxy spectral libraries. A star cluster of a given age defined the starburst spectral signature while a red galaxy nucleus represents a typical old metal-rich underlying population. The flux proportions for combining the spectra are dictated by three burst-to-galaxy mass ratios of 10%, 1%, and 0.1 %. In Fig. 5, solid, short-dashed, and long-dashed lines represent 10-%, 1-%, and 0.1-% burst masses, respectively.

BAS90 calculated Johnson *BVRI* colors from their synthesized spectra. We converted their starburst colors into the Cousins system via the following two formulae:

$$(V - R)_{\text{JC}} = \frac{1}{1.40} ((V - R)_{\text{J}} - 0.028) , \quad (V - R)_{\text{JC}} < 1.0 \quad (5)$$

$$(V - I)_{\text{JC}} = \frac{1}{1.30} ((V - I)_{\text{J}} - 0.013) , \quad (V - I)_{\text{JC}} < 2.0 \quad (6)$$

(Cousins 1976), and

$$(V - R)_{\text{JC}} = 0.73(V - R)_{\text{J}} - 0.03 , \quad (V - R)_{\text{J}} < 1.0 \quad (7)$$

$$(V - I)_{\text{JC}} = 0.778(V - I)_{\text{J}} - 0.03 , \quad (V - I)_{\text{J}} < 2.0 \quad (8)$$

(Bessell 1979). The converted colors derived from these two formulae agree within 0.01 mag. The tracks on Fig. 5 are the converted evolutionary loci. Furthermore, we need to estimate the internal extinction for comparison. As with Fig. 6, an applied reddening vector of $A_V = 0.1$ is shown in the upper left corner.

Figure 5 shows that most of the partial colors of our sample KUGs are located on the BAS90 model tracks, affirming the validity of applying this model to our measurements. We emphasize that the models are of a starburst superimposed on an old population, instead of the evolutionary models of the starburst component alone. Though we should keep in mind that the galaxy color is sensitive to the burst-mass fraction (BAS90) and metallicity of the gas (Leitherer & Heckman 1995), Both of which are rather uncertain, the important fact is that most of our sample KUGs have a young ($\lesssim 10^{7-8}$ yr) stellar component within their *old disks*, i.e. the star formation is taking place in the disks of the KUGs, not in their central regions.

We next examine the color distribution of the individual KUGs.

KUG 0908+451 This is a giant grand-designed spiral galaxy. The partial colors of the disk distribute around the 10^8 -yr phase of the 10-% burst mass track, or 10^7 -yr phase of the 1-% burst mass one. The symbol labeled 12 corresponds to the bulge of this galaxy. Clearly, the color of the bulge is red, implying a lack of a young population. The arm of the galaxy (labelled 23 in Fig. 5) is abundant in H II regions, and turns out to be the very blue color, corresponding to a stellar age of less than 10^7 yr of a 10-% burst mass.

KUG 0908+468 This galaxy is compact with the same color throughout. Comparison with the tracks indicates that the stellar ages of the burst component are $< 10^8$ yr, and burst mass ratio to the total baryonic mass is high ($>$ a few %), i.e. ongoing starburst occurs over the whole galaxy.

KUG 0911+471 This galaxy belongs to the giant spirals. The disk color is located around the 10^8 -yr phase of the 10-% burst mass track. The symbol labeled 6 represents the color of the bulge, which has a normal color for an old stellar population.

KUG 0919+474 This galaxy is compact, and like KUG 0908+468, has the same color throughout. The color of this galaxy can only be explained with a very high burst mass ratio, $\sim 10\%$. The implicated burst time is very recent ($10^6 \sim 10^7$ yr).

KUG 0924+448 This is a giant spiral galaxy with a variety of colors in the disk. Most of the disk color clusters around the 10^8 -yr phase of the $1 \sim 10\%$ burst mass tracks. Some other parts show colors corresponding to younger stellar populations. As with other giant spiral KUG samples, the bulge of this galaxy (labeled 20) is red.

KUG 0944+468 This is also a giant spiral galaxy, though it looks small in size because of its rather low surface brightness. Its bulge (labeled 4) is bluer than comparable KUG samples. But its disk parts are still bluer than the bulge. The color corresponds to a burst more recent than 10^8 -yr on the $1 \sim 10\%$ tracks.

KUG 0945+443 This is also a giant spiral galaxy. The dispersion of colors across the galaxy is large, implying that the ages of the SF regions on the disk range from 5×10^7 yr to 10^9 yr. The most crowded domain on the C-C diagram corresponds to the 10^8 -yr phase of the 10% or 1% burst mass tracks. Its bulge (labeled 12) is red, as expected from an old stellar component.

KUG 0947+445A This galaxy is a spiral, but has a rather strange shape consisting of four separate arms or two arms with a bar crossing between them. In addition, it is as small as a compact galaxy. Despite its morphological peculiarity, its disk parts have rather old stellar colors, corresponding to several $\times 10^8$ -yr phase of the $1 \sim 10\%$ burst mass tracks. Its bulge (labeled 5) has the same color as its disk parts, though the color is not so blue that it would be regarded as a nuclear starburst.

KUG 0953+466 This is a compact galaxy with a large dispersion in $(V - I)_T$. Its bursts correspond to a stellar age of $\sim 10^{6-7}$ yr with a burst mass fraction of several $\times 0.1$ %. The partial colors are well explained by this burst age and mass fraction, therefore the age dispersion may be also small as those of other compact KUG samples.

KUG 1007+461 This is a giant spiral galaxy. Its bulge (labeled 9) is slightly bluer than those of other spiral galaxy samples, and its disk components distribute around the domain of a very young stellar population. Suggested stellar age is around $10^7 \sim 10^8$ yr.

KUG 1016+467 This is the only interacting galaxy pair in our sample. The parent or larger one is a giant spiral galaxy. We show only the partial colors of the parent galaxy in Fig. 5. This galaxy has a large color dispersion across its disk, corresponding to a stellar population with an age of $10^7 \sim \text{several} \times 10^8$ yr superimposed on an old background population. Its bulge (labeled 13) is also somewhat blue.

5.3. Morphology

We have described the individual morphologies of the LUM-filament KUGs in section 4.2. In addition, the KUG catalog gives original morphological classification as follows (TM93): Ic is an irregular galaxy with clumpy HII regions, Ig is an irregular galaxy with a conspicuously giant HII region, Pi is a pair of interacting components, Pd is a pair of detached components, Sk is a spiral galaxy with knots of HII regions along its arms, Sp is a spiral galaxy with a peculiar bar and/or nucleus, C is a compact galaxy, and “?” is unclassifiable. The morphological properties of the objects in this study, as well as the originally cataloged KUG morphology and star formation properties are summarized in Table 8. Column 1 shows the KUG names. Column 2 presents the RC3 T indices for

each KUG. For the galaxies which RC3 T s are not given, we give our assigned indices instead. Unclassifiable compact galaxies are labeled “C”. We show the KUG morphological classification in column 3. The star formation properties are presented in columns 4 – 6; column 4 gives the location where star formation occurs within the galaxy, column 5 gives the derived ages of the superposing stellar population, and column 6 gives the burst-to-galaxy mass ratios of our samples. We note their morphological features in columns 7, 8, and 9. Our LUM-filament KUG sample are roughly divided into two classes, which are the class of knotty spirals Sk and the class of compact galaxies C. This is consistent with the morphological analysis based on our CCD images.

Despite the variety of morphologies, some general points are apparent:

1. Our sample KUGs are divided into two classes, giant spiral systems and compact galaxies.
2. Most of the giant-spiral KUGs show disk distortion.
3. Giant-spiral KUGs have highly developed arms and a knotty appearance due to giant HII regions.
4. In spite of 2 and 3, roughly half of our sample is isolated, and the other half has some companions, or lies in a group of galaxies.
5. Only one of our sample (KUG1016+467) shows explicit interaction features. This galaxy is an interacting system of a giant spiral and a small amorphous satellite.

One of the main conclusions of TTUS97 is that, in terms of stellar population, the late-type KUGs are mostly normal galaxies and the early-type KUGs often turned out to be peculiar galaxies. The color difference between the KUGs and non-KUGs is significant for $T < 5$, and indicates that the early-type KUGs have a young stellar population for their

morphologies. Compact galaxies tend to be included in the early-type galaxy classification as peculiar early-types and are thus not really a proper member of the class. On the other hand, though the spiral KUGs in our sample have a young stellar population in their disks which makes their appearance quite knotty, they are rather normal for their morphology. This is also consistent with the above result of TTUS97. The spiral KUG samples have no active nuclei or circumnuclear Starbursts. Therefore they are “active normal spirals”.

5.4. Correlation between Various Properties of our Samples

Here we examine the relation between the colors, ages, morphologies, and environments of our samples. Many authors have claimed a close connection between active star formation and morphological distortion. For example, BCD95 have performed a quantitative morphological analysis of their MBG starbursts by Fourier transforming the isophotes of sample galaxies. They concluded that the star formation regions associate with isophotal twists. Such distortion or twist from symmetry is also found in our KUG sample in the LUM filament. Z96 have discovered that a significant fraction of their “E+A” sample exhibits tidal features. But, as BCD95 has pointed out, the morphological distortion is not a direct evidence of galaxy-galaxy interaction. Half of our sample is isolated galaxies. Only one has a tidally-connected companion. Thus, we cannot attribute the starformation in our sample to distortion features, though galaxy encounters might be responsible for some of the starbursts.

We next consider the relations between the stellar ages implied by the color distribution and other properties. A clear morphological relation exists. Compact galaxies which have a featureless appearance have very young superposing stellar components ($10^6 \sim 10^7$ yr), i.e. on-going starbursts, spread over the whole galaxy. In contrast, giant spiral galaxies which have well-developed arms have more aged stellar components ($10^7 \sim 10^8$ yr) in their

disks, and their bulge is old. The age scatter is large in each spiral sample. But there is an exception, KUG0947+445A, which is a spiral galaxy but has a small dispersion of partial colors. We note that this is a physically small galaxy, as we saw in section 5.2. The color dispersion appears to correlate with galaxy size with larger galaxies having a greater dispersion.

Finally we look into the relation between the stellar age and existence of companions. The most active star forming galaxy is KUG 0919+474, which is a compact galaxy in a group having a burst age of $10^6 \sim 10^7$ yr. Isolated compact galaxy KUG 0908+468 also has rather young starbursts, but their ages are not as young as those of KUG 0919+474. Another isolated compact KUG 0953+466 has a burst age of $10^6 \sim 10^7$ yr, with a small burst mass fraction of (\sim several \times 0.1 %) implied. Spiral galaxies have similar stellar ages with each other. Some KUGs in a group or with companions have rather younger stellar ages, like KUG 1007+461 and KUG1016+467. In contrast, other KUGs with companions have the superposing stellar components consistent with intermediate ages, like KUG 0945+443 and KUG 0947+445A. Thus, there is no clear relation between the superposing stellar age and the existence of companions.

6. SUMMARY

We have focused on the collective star formation enhancement of galaxies, and searched for the regions where such phenomena have occurred using the Kiso Ultraviolet-excess Galaxy (KUG) catalog as a SF-enhanced galaxy sample. Through our survey we found four KUG-rich regions, one of which turned out to be associated with a filamentary structure. We named it “the Lynx-Ursa Major (LUM) filament” after its location on the sky ($\alpha \sim 9^{\text{h}} - 10^{\text{h}}$, $\delta \sim 42^\circ - 48^\circ$). We then investigated the star formation properties of the KUGs in the LUM. Our results are as follows:

1. The eleven KUG objects we examined in the LUM filament proved to be generally blue by CCD photometry, and they show a much larger scatter on C-C diagrams than that of normal galaxies. This is similar to those of other UV-excess galaxy surveys, such as the Markarian survey, or MBG survey.
2. The spiral subset of the sample has conspicuous HII-region knots in their arms. The rest are compact galaxies with no structure and an extremely blue color. We suggest that the former corresponds to the KUG subset of “normal late-type spiral galaxies”, and the latter corresponds to the “peculiar early-type galaxies”, proposed by TTUS97.
3. The star formation of our sample KUGs occurs in the whole disk, and is not concentrated in the central regions. This is different from those of SBNGs which are the main constituent of The MBG survey. None of our sample KUGs have nuclear activity. The age of their young stellar population is $\lesssim 10^{7-8}$ yr. Compact samples have very young superposing stellar components ($10^6 \sim 10^7$ yr) spread over the whole galaxy, while giant spiral samples have moderately aged stellar components ($10^7 \sim 10^8$ yr) in their disks, and an older bulge. The age scatter is large in each spiral sample. Star formation properties of giant spiral samples and compact samples are clearly different, implying that the star formation is regulated by the inner galaxy environment.
4. Only one KUG exhibits an explicit interaction feature, although half of our sample have some companions. However, most of the spiral subset of our sample show distortions or isophotal twists. This indicates that a weak encounter may have activated the star formation, though we should note that their morphological distortion is not necessarily due to an external force.
5. The age and strength of star formation in individual samples has no relation to the existence of companions, implying that star formation may not be activated by the

local environment.

We should also note that there are no extremely peculiar galaxies in this region. A detailed spatial distribution of KUGs and non-KUGs in the LUM filament should be investigated in order to further study the effects of environment. A redshift survey to study the detailed spatial distribution of KUGs is now in progress, the results of which will appear in Takeuchi et al. (1998).

We first offer our thanks to the referee, Dr. J. W. Moody whose comments greatly helped in improving the clarity and English presentation of this work. We would like to thank Daisaku Nogami, Adel T. Roman, and Tadahiro Manmoto, as well as Kiso Observatory staff members for helping with observations. We also thank Masaru Hamabe for giving us the latest version of SPIRAL. One of us (TTT) is grateful to Kouji Ohta, Takashi Ichikawa, Ichi Tanaka, Youichi Ohyama, and Shingo Nishiura for giving a great deal of useful suggestions and discussions. TTT also acknowledges the Research Fellowships of the Japan Society for the Promotion of Science for Young Scientists. This research has made use of the NASA/IPAC Extragalactic Database (NED) which is operated by the Jet Propulsion Laboratory, California Institute of Technology, under contract with the National Aeronautics and Space Administration. We also gratefully acknowledge the NASA's Astrophysics Data System Abstract Service (ADS).

REFERENCES

- Augarde, R., Chalabaev, A., Comte, G., & Maehara, H. 1994, *A&AS*, 104, 259
- Barth, C. S., Coziol, R., & Demers, S. 1995, *MNRAS*, 276, 1224 (BCD95)
- Bessell, M. S. 1979, *PASP*, 91, 589
- Bica, E., Alloin, D., & Schmidt, A. 1990, *MNRAS*, 242, 241
- Burstein, D., & Heiles, C. 1982, *AJ*, 87, 1165
- Buta, R., & Williams, K. L. 1995, *AJ*, 109, 543
- Cardelli, J. A., Clayton, C. C., & Mathis, J. S. 1989, *ApJ*, 345, 245
- Comte, G., Augarde, R., Chalabaev, A., Kunth, D., & Maehara, H. 1994, *A&A*, 285, 1
- Cousins, A. W. F. 1976, *MemRAS*, 81, 25
- Coziol, R., Demers, S., Barnéoud, R., & Peña, M. 1997, *AJ*, 113, 1548
- Coziol, R., Demers, S., Peña, M., Torres-Peimbert, S., Fontaine, G., Wesemael, F., & Lamontagne, R. 1993, *AJ*, 105, 35
- de Lapparent, V., Geller, M. J., & Huchra, J. P. 1986, *ApJ*, 302, L1
- de Vaucouleurs, G., de Vaucouleurs, A., Corwin, H. G., Jr., Buta, R. J., Paturel, G., & Fouqué, P. 1991, *Third Referencd Catalogue of Bright Galaxies Vols. I – III*, Springer-Verlag, New York (RC3)
- Dressler, A., & Gunn, J. E. 1983, *ApJ*, 270, 7
- Fairall, A. 1998, *Large-scale Structures in the Universe*, John Wiley & Sons Ltd., West Sussex

- Geller, M. J., & Huchra, J. P. 1989, *Science*, 246, 897
- Giovanelli, R., & Haynes, M. P. 1982, *AJ*, 87, 1355
- Hamabe, M., & Ichikawa, T. 1992, in *Proceedings of Astronomical Data Analysis Software and System I*. ASP Conf. 25, D. Worrall, et al. eds., ASP, San Francisco, p.325
- Han, C., Gould, A., & Sackett, P. D. 1995, *ApJ*, 445, 46
- Horaguchi, T., Ichikawa, S., Yoshida, M., Yoshida, S., & Hamabe, M. 1994, *Publ. Natl. Astr. Obs. Japan*, 4, 1
- Huchra, J. P. 1977, *ApJS*, 35, 171
- IRAS Faint Source Catalog*, 1988, Joint *IRAS Science Working Group*, Washington, DC:GPO
- Kirshner, R. P., Oemler, A., Jr., & Schechter, P. L. 1978, *AJ*, 83, 1549
- Kodaira, K., Okamura, S., & Ichikawa, S. 1990, *Photometric Atlas of Northern Bright Galaxies*, University of Tokyo Press, Tokyo
- Landolt, A. U. 1992, *AJ*, 104, 372
- Larson, R. B., & Tinsley, B. M. 1978, *ApJ*, 219, 46
- Leitherer, C. & Heckman, T. M. 1995, *ApJS*, 96, 9
- Maehara, H., Inoue, M., Takase, B., & Noguchi, T. 1985, *PASJ*, 37, 451
- Maehara, H., Noguchi, T., Takase, B., & Handa, T. 1987, *PASJ*, 39, 393
- Maehara, H., Hamabe, M., Bottinelli, L., Gouguenheim, L., Heidmann, J., & Takase, B. 1988, *PASJ*, 40, 47

- Maia, M. A. G., Pastoriza, M. G., Bica, E., & Dottori, H. 1994, *ApJS*, 93,425
- Markarian, B. E., Lipovetsky, V. A., Stepanian, J. A., Erastova, L. K., & Shapovalova, A. I. 1989, *Comm. Special Astrophys. Obs.*, 62, 5
- Menzies, J. W., Marang, F., Laing, J. D., Coulson, I. M., & Engelbrecht, C. A. 1991, *MNRAS*, 248, 642
- Miyauchi-Isobe, N., Takase, B., & Maehara, H. 1997, *Publ. Natl. Astr. Obs. Japan*, 4, 153
- Pastoriza, M. G., Bica, E., Maia, M. A. G., Bonatto, Ch., & Dottori, H. 1994, *ApJ*, 432, 128
- Schechter, P. L. 1976, *ApJ*, 203, 297
- Takamiya, M., Kron, R. G., & Kron, G. E. 1995, *AJ*, 110, 1083
- Takase, B. 1980, *PASJ*, 32, 605
- Takase, B., & Miyauchi-Isobe, N. 1993, *Publ. Natl. Astr. Obs. Japan*, 3, 169 (TM93)
- Takata, T., Ichikawa, S., Horaguchi, T., Yoshida, M., Yoshida, S., Ito, T., Nishihara, E., & Hamabe, M. 1995, *Publ. Natl. Astr. Obs. Japan*, 4, 9
- Takeuchi, T. T., Nakanishi, K., Hirashita, H., Ishii, T. T., Nomura, H., Saitō, M., Tomita, A., & Iwata, I. 1998, in preparation
- Tomita, A., Tomita, Y., & Saitō, M. 1996, *PASJ*, 48, 285
- Tomita, A., Takeuchi, T. T., Usui, T., & Saitō, M. 1997, *AJ*, 114, 1758 (TTUS97)
- Tomita, A., Maehara, H., Takeuchi, T. T., Nakanishi, K., Honma, M., Tutui, Y., & Sofue, Y. 1998, *PASJ*, submitted

Zabludoff, A. I., Zaritsky, D., Lin, H., Tucker, D., Hashimoto, Y., Sheckman, S. A., Oemler, A., Jr., & Kirshner, R. P. 1996, *ApJ*, 466, 164 (Z96)

Zwicky, F., Herzog, E., Karpowicz, M., Kowal, C. T., & Wild, P. 1961 – 68, *Catalogue of Galaxies and of Clusters of Galaxies Vols. I – VI*, California Institute of Technology, Pasadena (CGCG)

FIGURE CAPTIONS

Figure 1 – The distribution of the fraction of Kiso Ultraviolet-excess galaxies (KUGs) f_{KUG} relative to the number density of CGCG galaxies n . Each symbol represents f_{KUG} in a $6^\circ \times 6^\circ$ -area. The confidence limits of 99.9 %, 99.99 %, and 99.999 % are also shown. The filled symbols, all outside the 99.99 % envelop represent the KUG-rich regions. Eight filled symbols are plotted, but some of them (B and one of Ds, and C and one of Es) are overlapping with each other, and consequently the number of filled symbols appears as six. The regions which have the same labels are adjacent to each other on the sky.

Figure 2 – All-sky projection map of the KUG-rich regions. The small dots represent the distribution of CGCG galaxies in KUG-survey regions, and the black hatches depict the KUG-rich regions. The labels A, B, C, D, and E attached to the black-hatched regions correspond to the labels in Fig. 1.

Figure 3 – Contour maps in the V - and I_C -bands of the objects in our sample. They are shown from top to bottom in increasing order of right ascension. Each contour interval is 0.5 magnitudes. In this figure, the north is above, and the east to the right. The FOV of the contour maps is $2'.5 \times 2'.5$. A distance scale is presented in the upper-left of each galaxy image.

Figure 4 – The photometric partitioning of each galaxy image.

Figure 5 – Color-color (C-C) diagrams of each square section of each galaxy shown in Fig. 4. The data points labeled “bulge” and “disk” represent the color of bulge and disk sections of the object respectively. The three broken lines on the C-C diagrams are the model starburst evolutionary tracks superimposed on an older stellar population, given by Bica, Alloin, & Schmidt (1990).

Figure 6 – The $(V - R)_T^0 - (V - I)_T^0$ diagram, comparing the dereddened total colors of our KUGs in the Lynx-Ursa Major filament with those covering the galaxy morphology sequence. Open circles represent the mean color of each morphological type index T . The shown indices are $-5, -4, -3, -2, -1, 0, 1, 2, 3, 4, 5, 6, \{7 \text{ and } 8\}, 9,$ and 10 , from Buta & Williams (1995) and some are labeled to show the trend. Error bars show the standard deviation of the color of galaxies in each morphological type. Filled squares represent the dereddened color of our KUGs. A vector showing the effect of the applied $A_V \sim 0.15$ reddening correction is presented in the top left of the diagram. A typical photometric error of our data is shown in the bottom right. The numbers beside the filled squares are the morphological type indices of the KUGs. We give the symbol “C” to compact galaxies instead of the T -index. Our sample tends to deviate from the range of the 1σ -strip of the Hubble sequence.

TABLE 1 : KUG-RICH REGIONS

Label	R.A.	Dec.	KUG field No(s). ^a
A	9 ^h ~ 10 ^h	42° ~ 48°	0286, 0287, 0288
B	~ 12 ^h	36° ~ 42°	0352, 0353, 0354
C	7 ^h ~ 8 ^h	30° ~ 36°	0405, 0406
D	~ 13 ^h	18° ~ 24°	0637

^a These are the original Kiso fields corresponding to the KUG-rich regions. Thus the locations and areas of them are slightly different from those shown in Fig. 1.

TABLE 2 : LYNX-URSA MAJOR FILAMENT

Location (α, δ)	$9^{\text{h}} - 10^{\text{h}}, 42^{\circ} - 48^{\circ}$
Projected Area ^a	$\sim 90 \text{ deg}^2$
Velocity Range cz	$2000 \text{ km s}^{-1} - 8000 \text{ km s}^{-1}$
Number of CGCGs n	~ 120
Number of KUGs k	~ 70
Fraction of KUGs f_{KUG}	$\sim 67 \%$

^a The filament extends east and west from the $6^{\circ} \times 6^{\circ}$ region A. In the adjacent regions, KUG fractions are also significantly high at The $\gtrsim 99.9 \%$ confidence level.

TABLE 3 : SELECTED KUGs AND THEIR BASIC PROPERTIES

No.	KUG name	CGCG name	$\alpha_{1950.0}$			$\delta_{1950.0}$			cz^a km s ⁻¹	$B_T^0{}^b$ mag	M_B^c mag
			h	m	s	°	'	"			
1	0908+451	0909.0+4510	9	8	55.7	45	9	39	2638	12.14	-19.96
2	0908+468	0908.4+4651	9	8	18.0	46	50	42	4287	14.50	-18.66
3	0911+471	0911.6+4707	9	11	34.5	47	6	38	4242	14.20	-18.94
4	0919+474	0919.0+4727	9	19	5.0	47	27	28	9121	15.77	-19.03
5	0924+448	0925.0+4453	9	24	55.1	44	52	56	7717	14.18	-20.26
6	0944+468	0944.2+4651	9	44	7.1	46	50	31	4708	14.74	-18.62
7	0945+443	0945.5+4418	9	45	34.2	44	18	49	4786	13.30	-20.10
8	0947+445A	0947.0+4432	9	47	1.8	44	31	43	4666	14.52	-18.83
9	0953+466	0953.6+4642	9	53	32.6	46	41	57	4681	15.15	-18.20
10	1007+461	1007.8+4612	10	07	48.4	46	11	49	7291	14.40	-19.91
11	1016+467	1016.0+4643	10	16	0.7	46	42	21	9169	14.10	-20.71

a Galactocentric velocities based on the value taken from the NED.

b B_T^0 -magnitudes from RC3.

c M_B for $h = 1.0$.

TABLE 4 : OBSERVATION LOG

KUG name	Date	Frame ID ^a
0908+451	1996 Nov 25	36782 ~ 36790
0908+468	1996 Nov 28	37087 ~ 37095
0911+471	1996 Nov 28	37099 ~ 37107
0919+474	1996 Nov 27	36971 ~ 36979
0924+448	1996 Nov 28	37061 ~ 37069
0944+468	1996 May 27	31375 ~ 31383
0945+443	1996 May 27	31387 ~ 31395
0947+445A	1996 Jun 1	31622 ~ 31630
0953+466	1996 Nov 27	36959 ~ 36967
1007+461	1996 Nov 28	37111 ~ 37119
1016+467	1996 Jun 1	31634 ~ 31642

a Frame ID numbers of the objects used in our paper. The actual name is of the form kcc36782, and here we omit the prefix “kcc”. Quick looks of the raw data of our observations are available on the World Wide Web through the Mitaka-Okayama-Kiso data Archival system (MOKA) at <http://www.moka.nao.ac.jp>. MOKA is operated by Astronomical Data Analysis Center, Okayama Astrophysical Observatory (National Astronomical Observatory of Japan) and Kiso Observatory (University of Tokyo) in cooperation with the Japan Association Information Processing in Astronomy (Horaguchi et al. 1994; Takata et al. 1995).

TABLE 5 : TOTAL MAGNITUDES BY GROWTH-CURVE FITTING

KUG name	V	R_C	I_C	M_V	M_R	M_I
	mag			+ 5 log h mag		
0908+451	11.54	11.01	10.63	−20.65	−21.16	−21.51
0908+468	13.97	13.56	13.22	−19.28	−19.67	−19.98
0911+471	13.47	12.99	12.56	−19.76	−20.22	−20.62
0919+474	15.28	14.88	14.63	−19.61	−19.99	−20.21
0924+448	13.49	13.02	12.58	−21.04	−21.49	−21.90
0944+468	14.36	13.96	13.51	−19.09	−19.47	−19.89
0945+443	12.61	12.17	11.72	−20.88	−21.30	−21.72
0947+445A	13.88	13.39	12.91	−19.56	−20.03	−20.48
0953+466	14.59	14.10	13.68	−18.85	−19.32	−19.71
1007+461	13.73	13.32	12.98	−20.67	−21.06	−21.37
1016+467	13.68	13.28	12.90	−21.22	−21.60	−21.95

TABLE 6 : COMPARISON OF OUR RESULT WITH LITERATURE

Object	Band	Our Photometry	Huchra 1977
KUG0953+466	V	14.96 ± 0.03	14.92 ± 0.05
	R_C	14.46 ± 0.03	14.41 ± 0.03

TABLE 7 : INTEGRATED COLORS

KUG name	$(V - R_C)_T$	$(V - I_C)_T$	$(R_C - I_C)_T$
0908+451	0.51	0.86	0.35
0908+468	0.39	0.70	0.31
0911+471	0.46	0.86	0.40
0919+474	0.38	0.60	0.22
0924+448	0.45	0.85	0.41
0944+468	0.38	0.80	0.42
0945+443	0.42	0.84	0.42
0947+445A	0.48	0.92	0.45
0953+466	0.47	0.85	0.39
1007+461	0.39	0.71	0.31
1016+467	0.39	0.73	0.35

TABLE 8: SUMMARY ON MORPHOLOGY AND STAR FORMATION CHARACTERISTICS

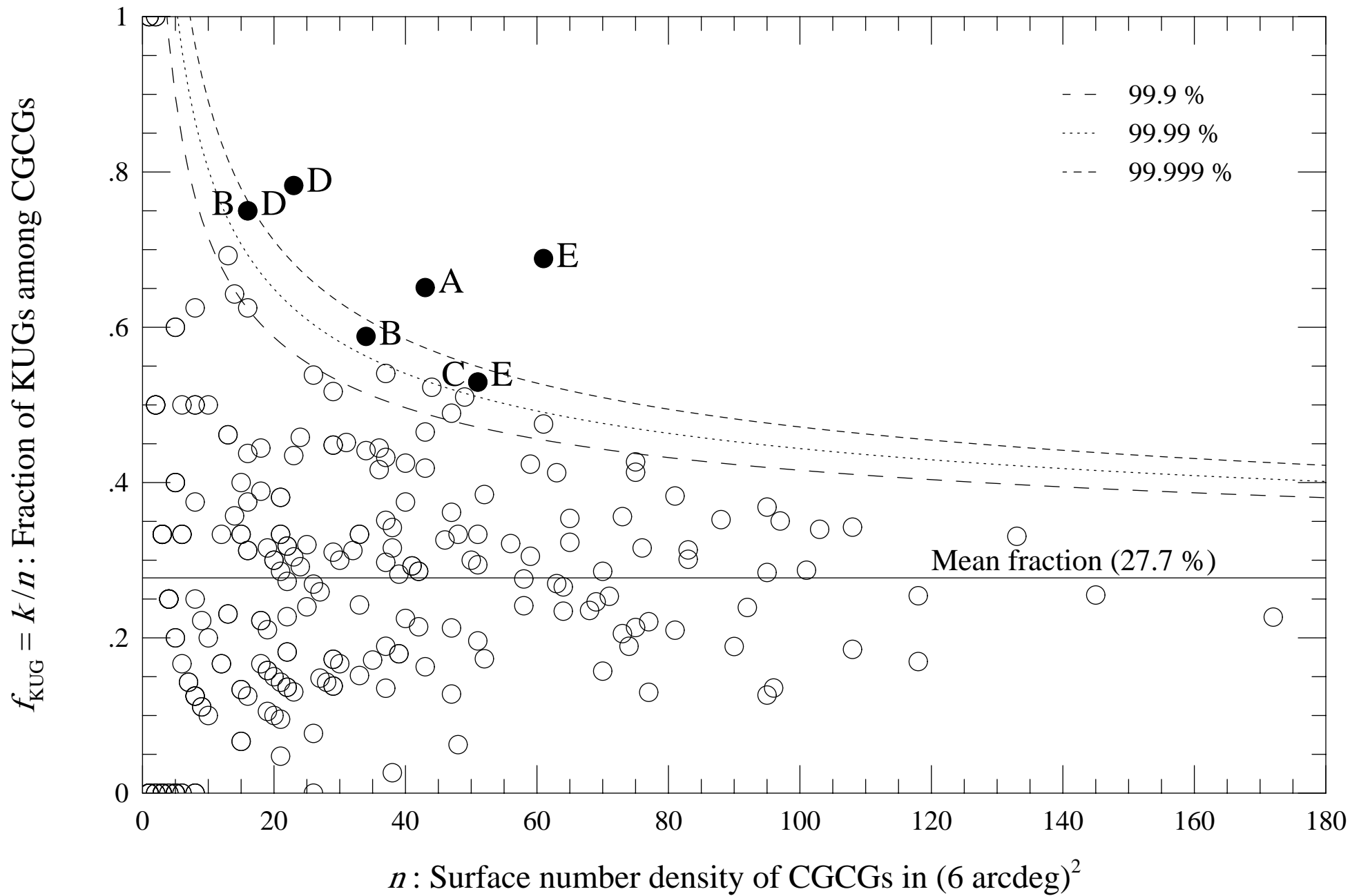
KUG name	Type		SF ^a	Age ^b [yr]	Burst [%]	Notes		
	<i>T</i>	KUG				Appearance	Distortion	Environment
0908+451	5	Sk	Disk	10 ^{7–8}	1 – 10	Knotty	Yes	Isolated
0908+468	C ^c	C	Whole	10 ⁷	10	Featureless	–	Isolated
0911+471	5 ^d	Sk	Disk	10 ⁸	10	Knotty	Yes	Isolated
0919+474	C ^c	C	Whole	10 ^{6–7}	10	Featureless	–	In a group
0924+448	5	Sk	Disk	10 ⁸	1 – 10	Knotty	Yes (triple-armed)	Isolated
0944+468	6	Sk	Disk	10 ^{7–8}	1 – 10	Knotty	Yes	Isolated
0945+443	5	Sk	Disk	10 ⁸	10	Knotty	–	In a group
0947+445A	4 ^d	Sp:	Disk	10 ^{8–9}	1 – 10	Smooth	– (four-armed)	In a group
0953+466	C ^c	C	Whole	10 ^{6–7}	≲ 1	Featureless	–	Isolated
1007+461	5 ^d	Sk	Disk	10 ^{7–8}	10	Smooth	–	Companion
1016+467	4	Pi:	Disk	10 ^{7–8}	10	–	Yes (tidal feature)	Inteacting

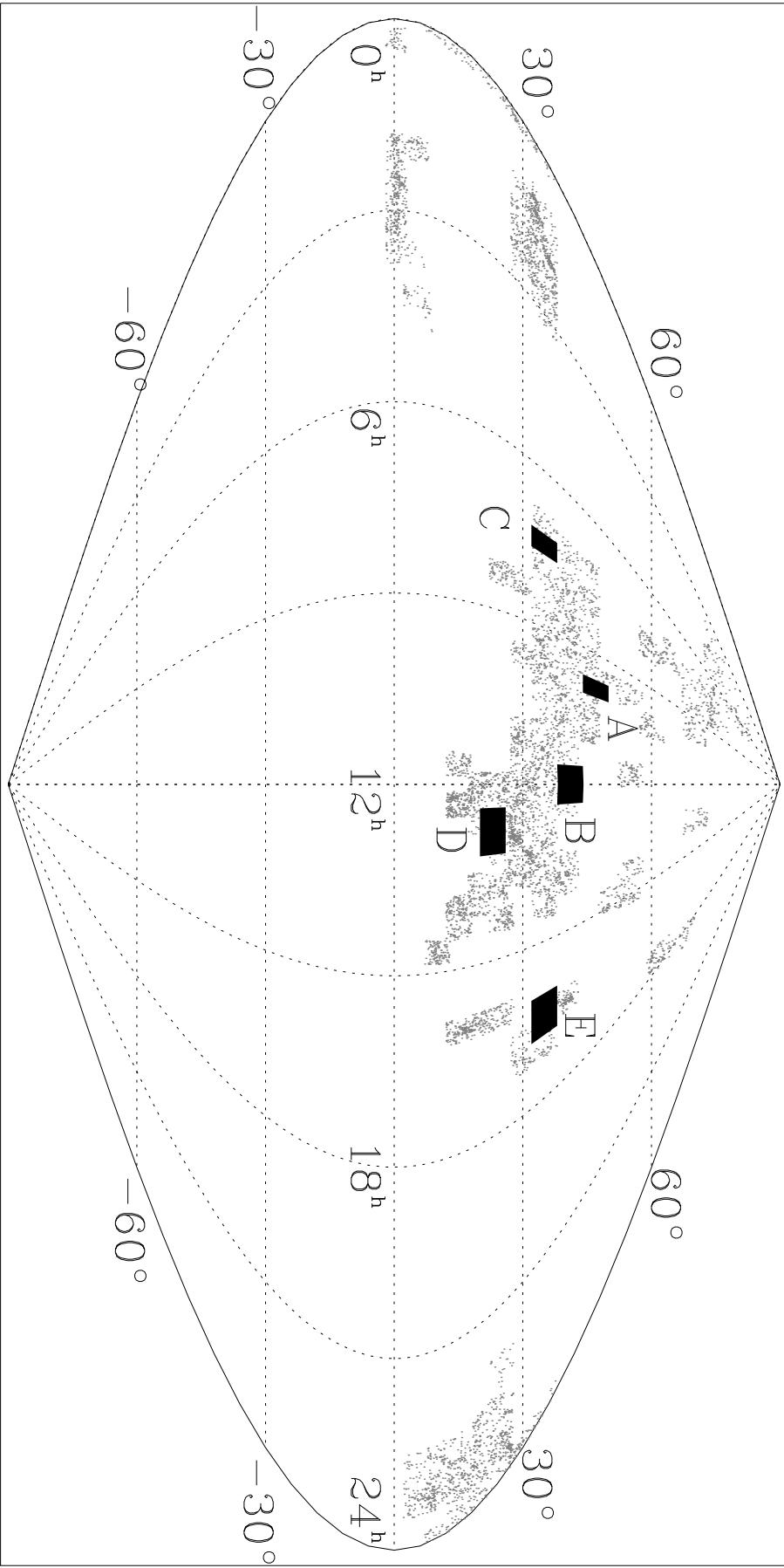
a Location where active star formation occurs on the galaxy.

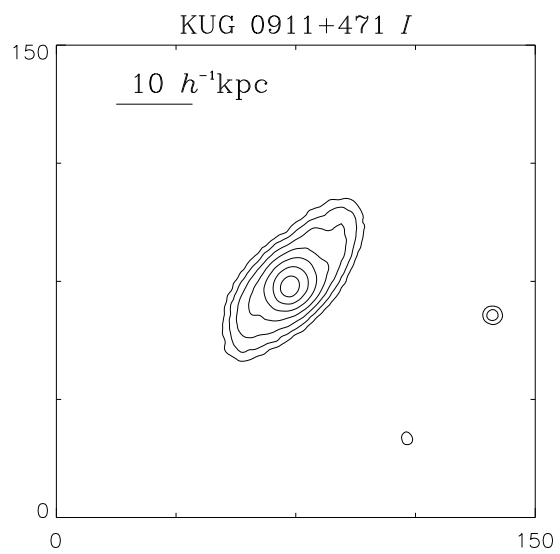
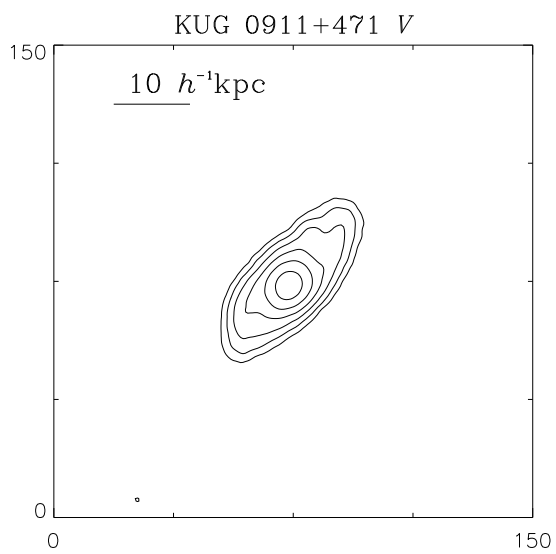
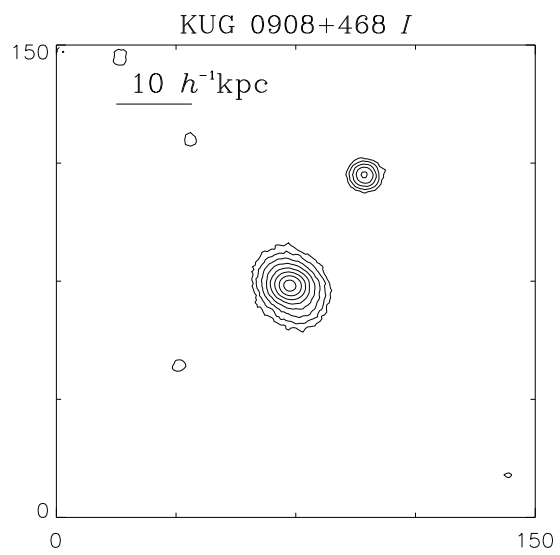
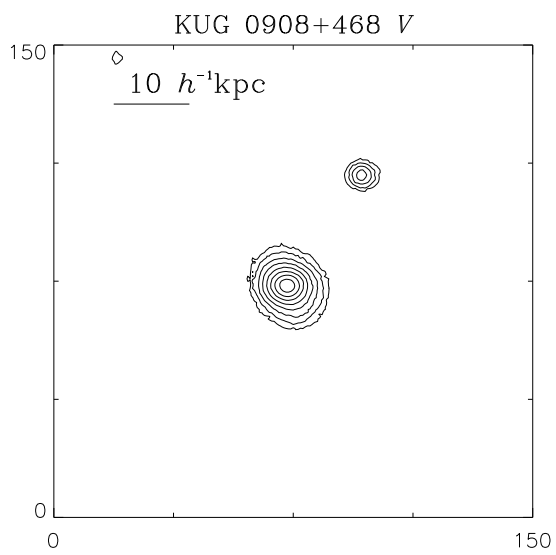
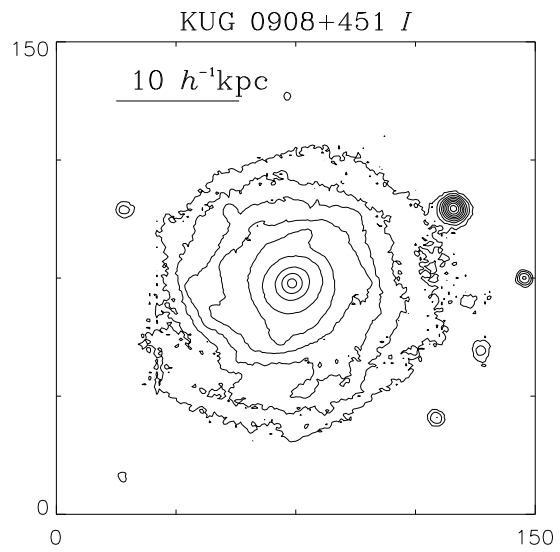
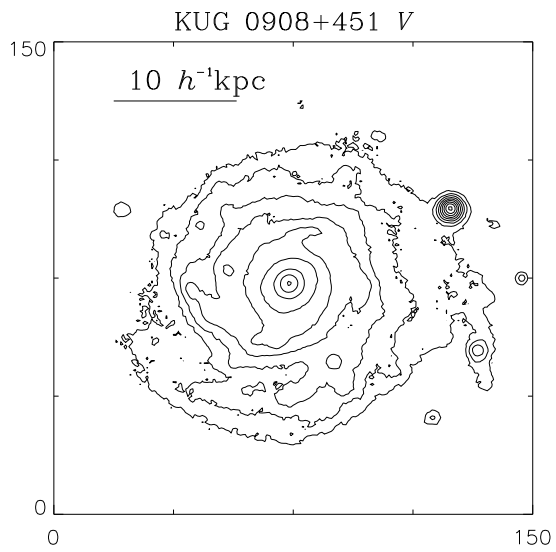
b Burst-to-galaxy mass ratio based on Bica et al. (1990).

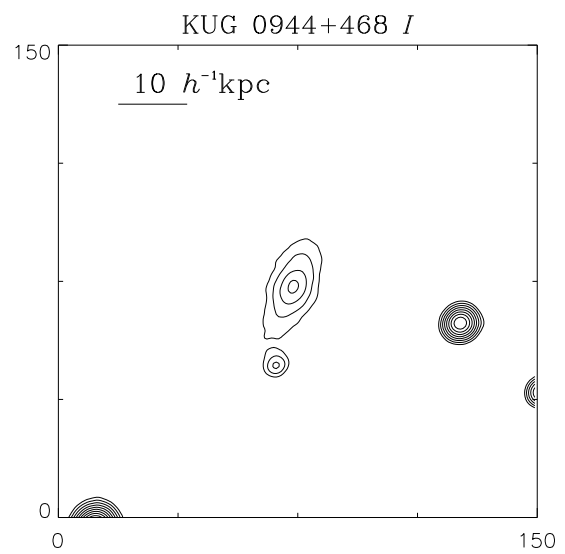
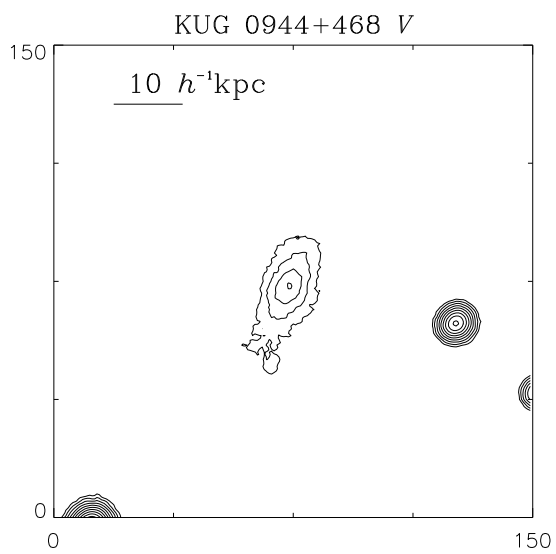
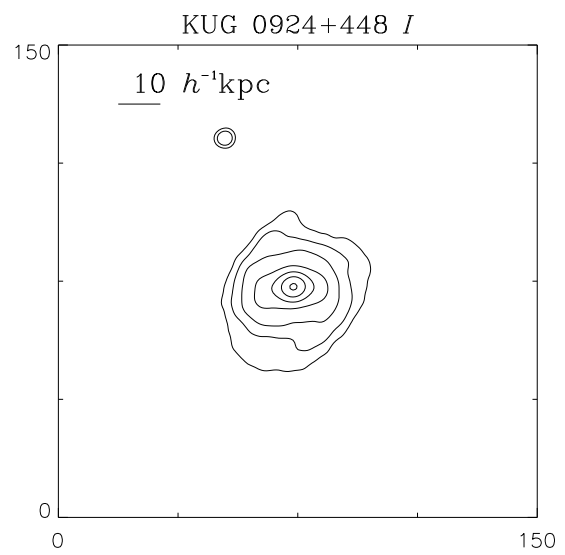
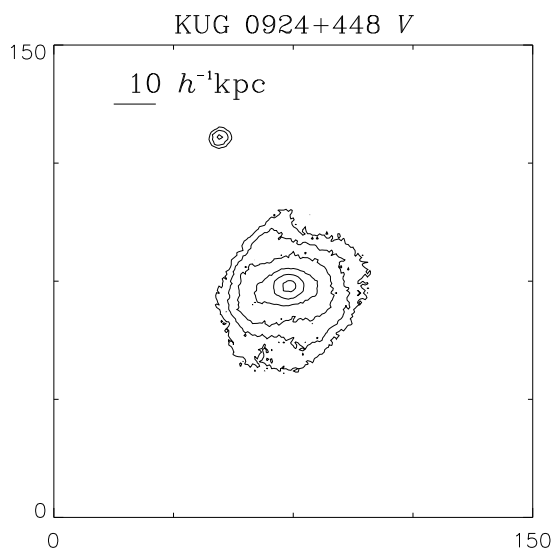
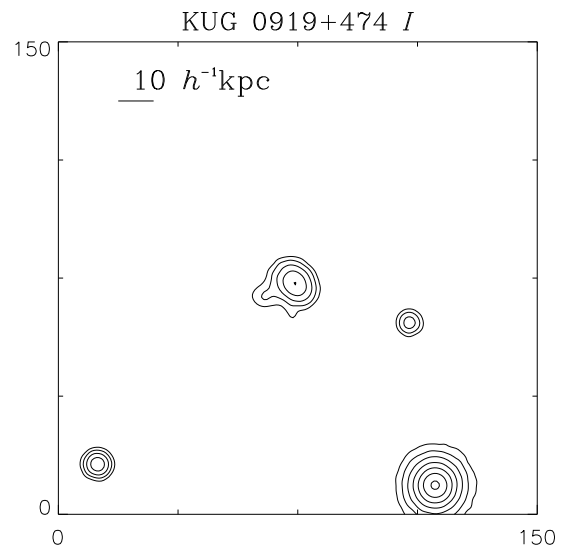
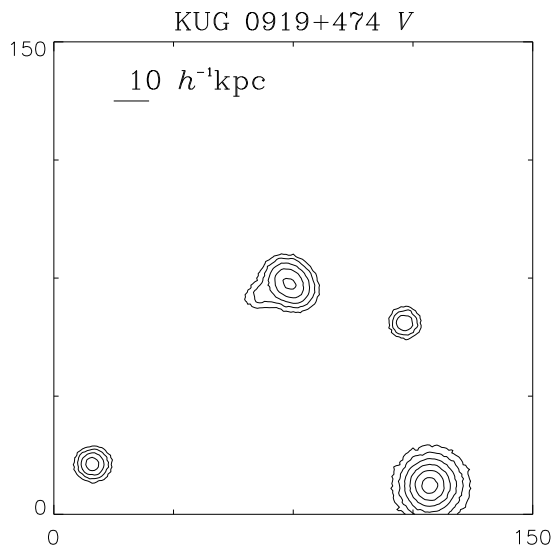
c Not given in RC3, and has featureless compact morphology.

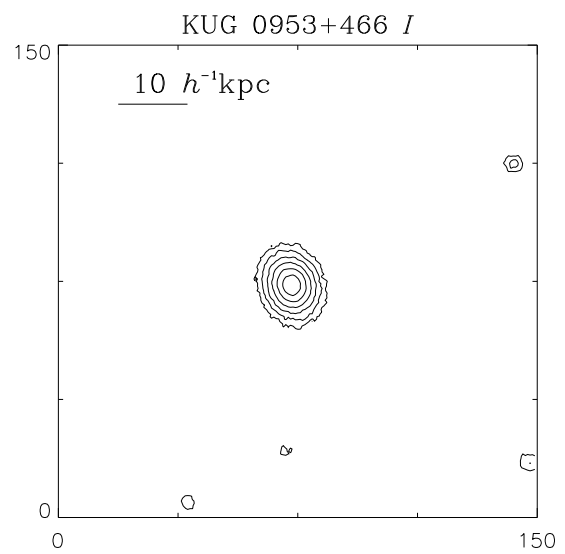
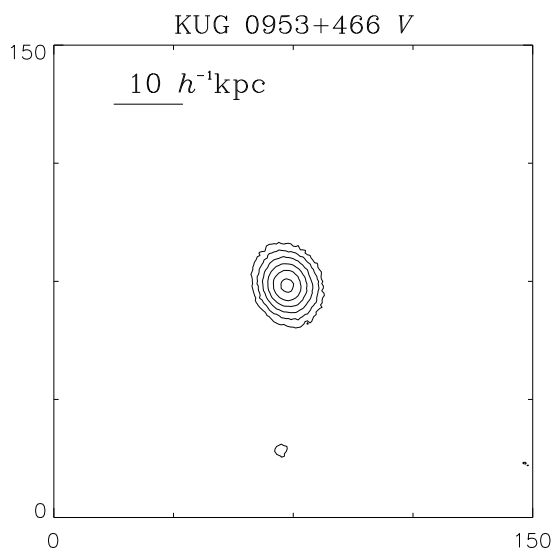
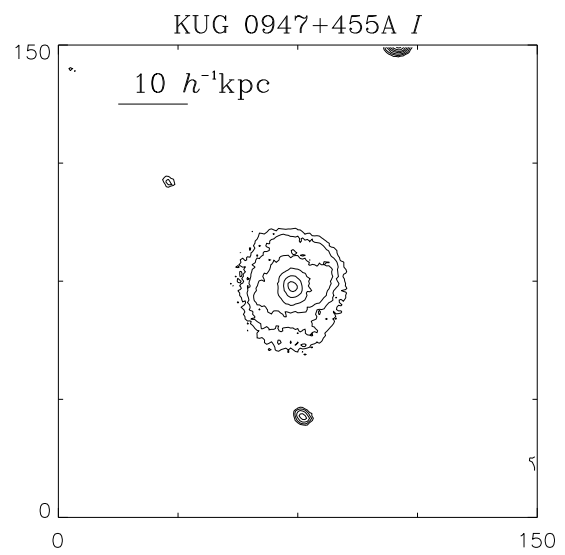
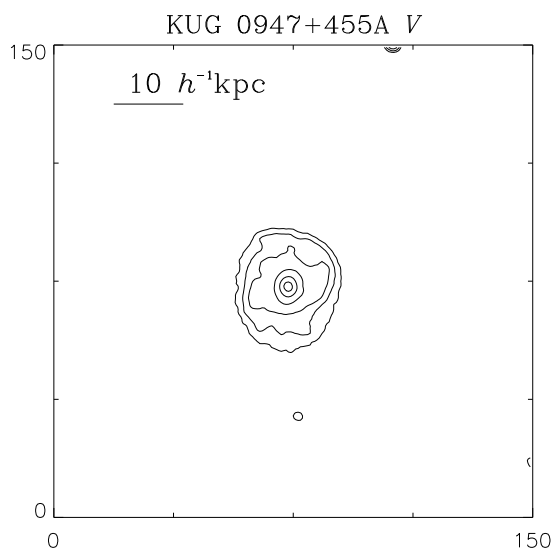
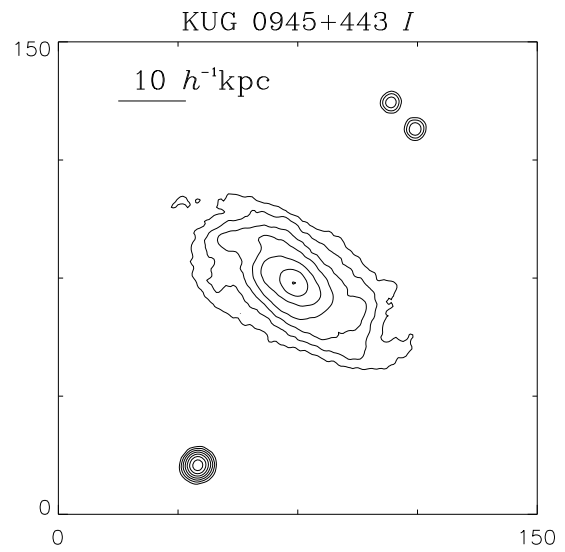
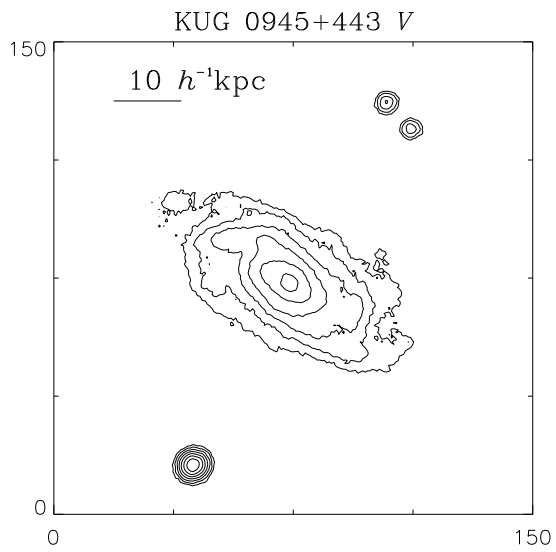
d Not given in RC3. Assigned by us.

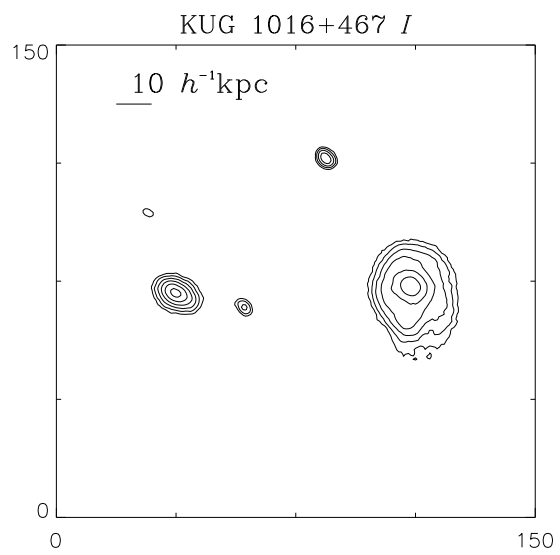
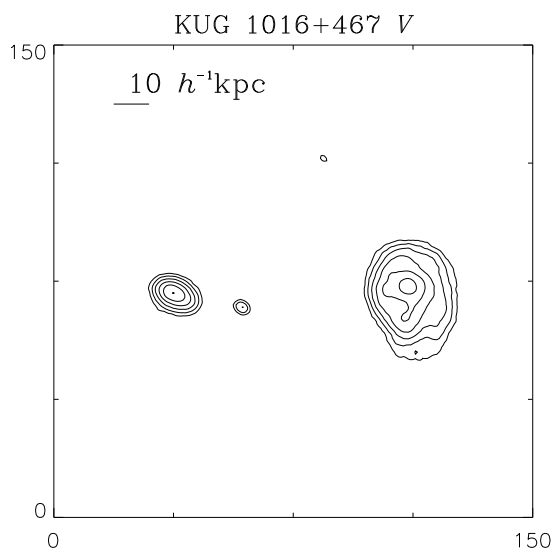
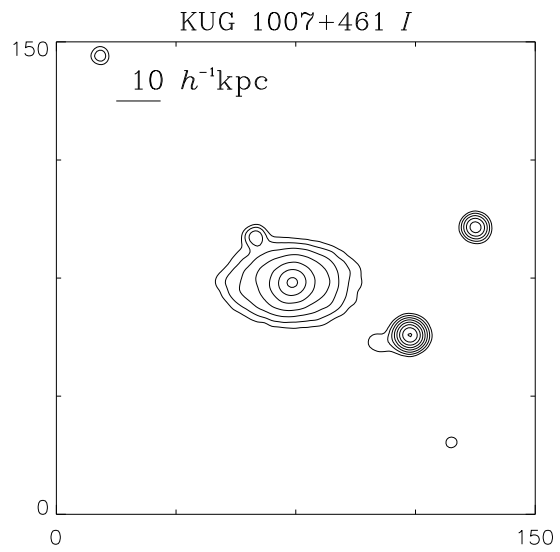
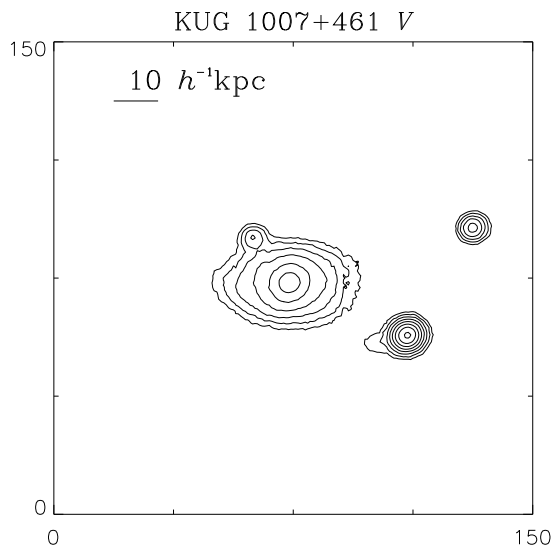




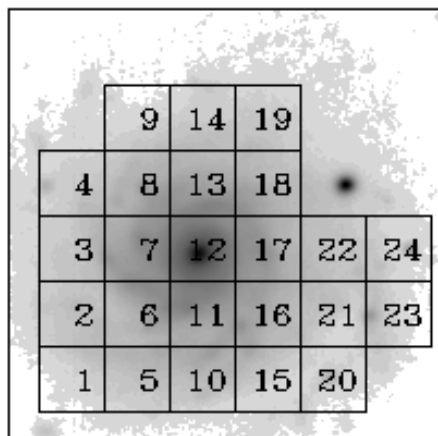




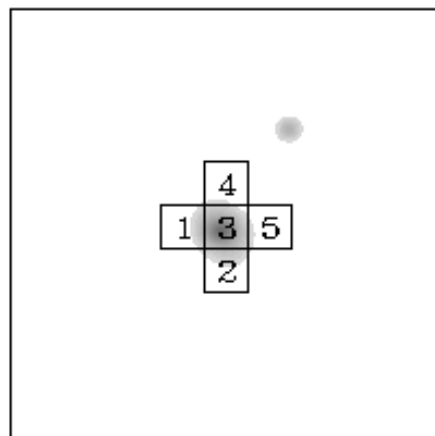




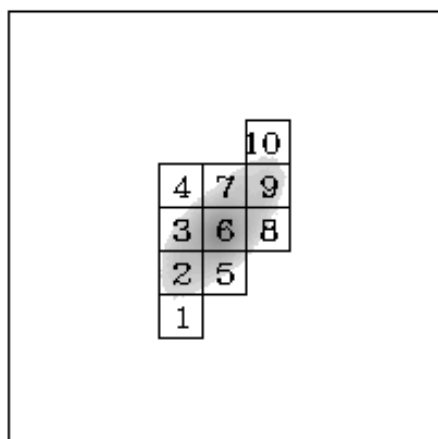
KUG 0908+451



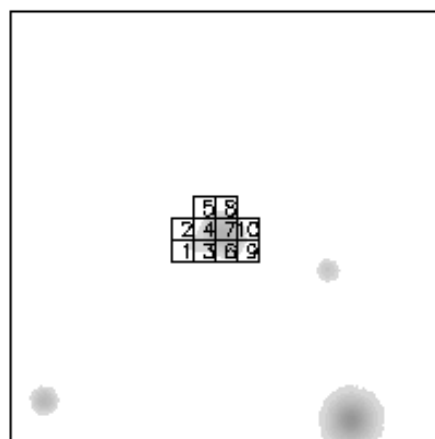
KUG 0908+468



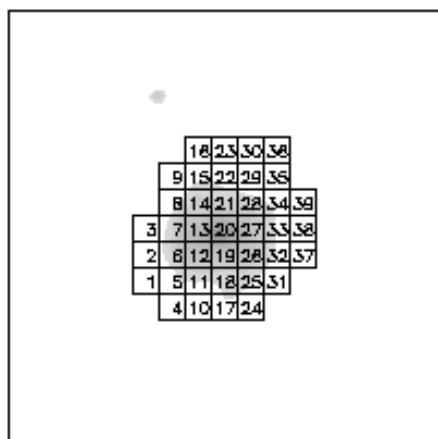
KUG 0911+471



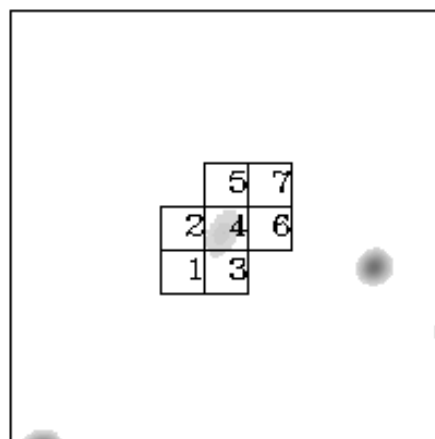
KUG 0919+474



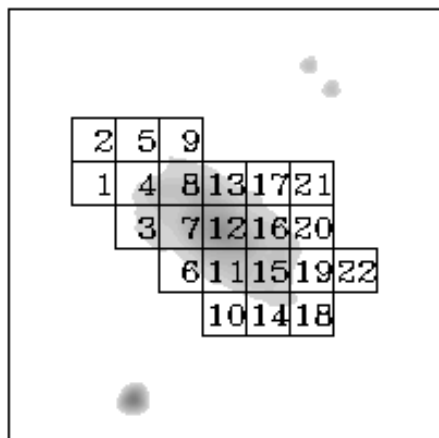
KUG 0924+448



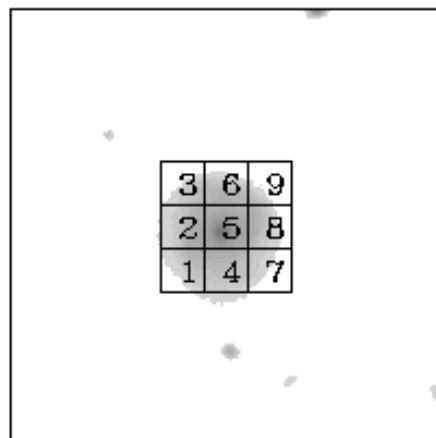
KUG 0944+468



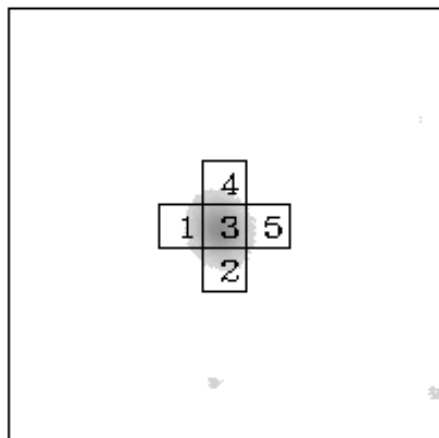
KUG 0945+443



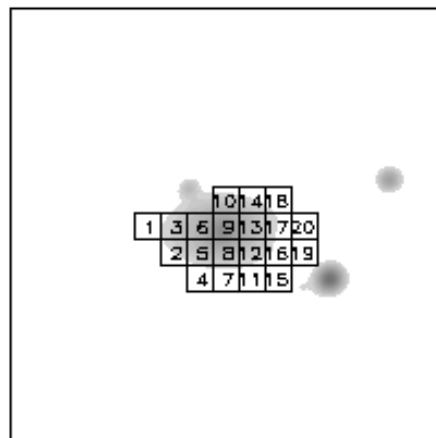
KUG 0947+445A



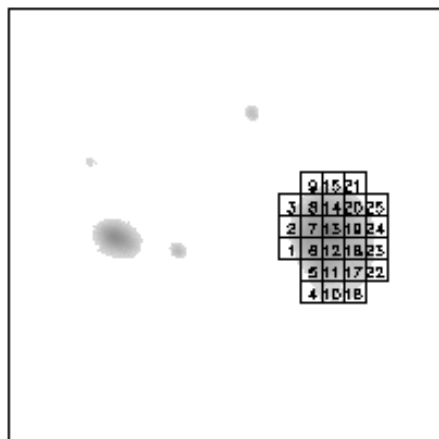
KUG 0953+466



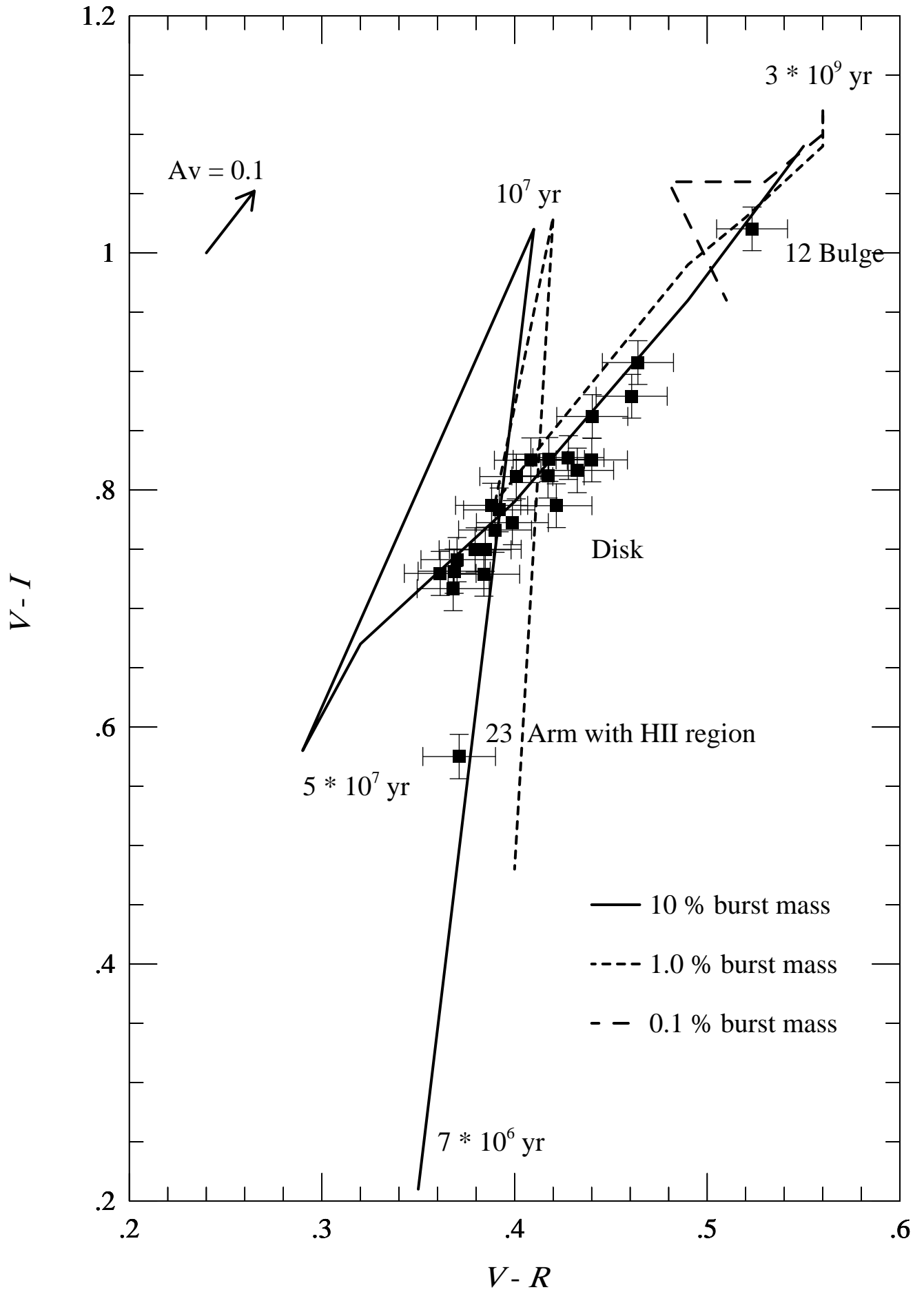
KUG 1007+461



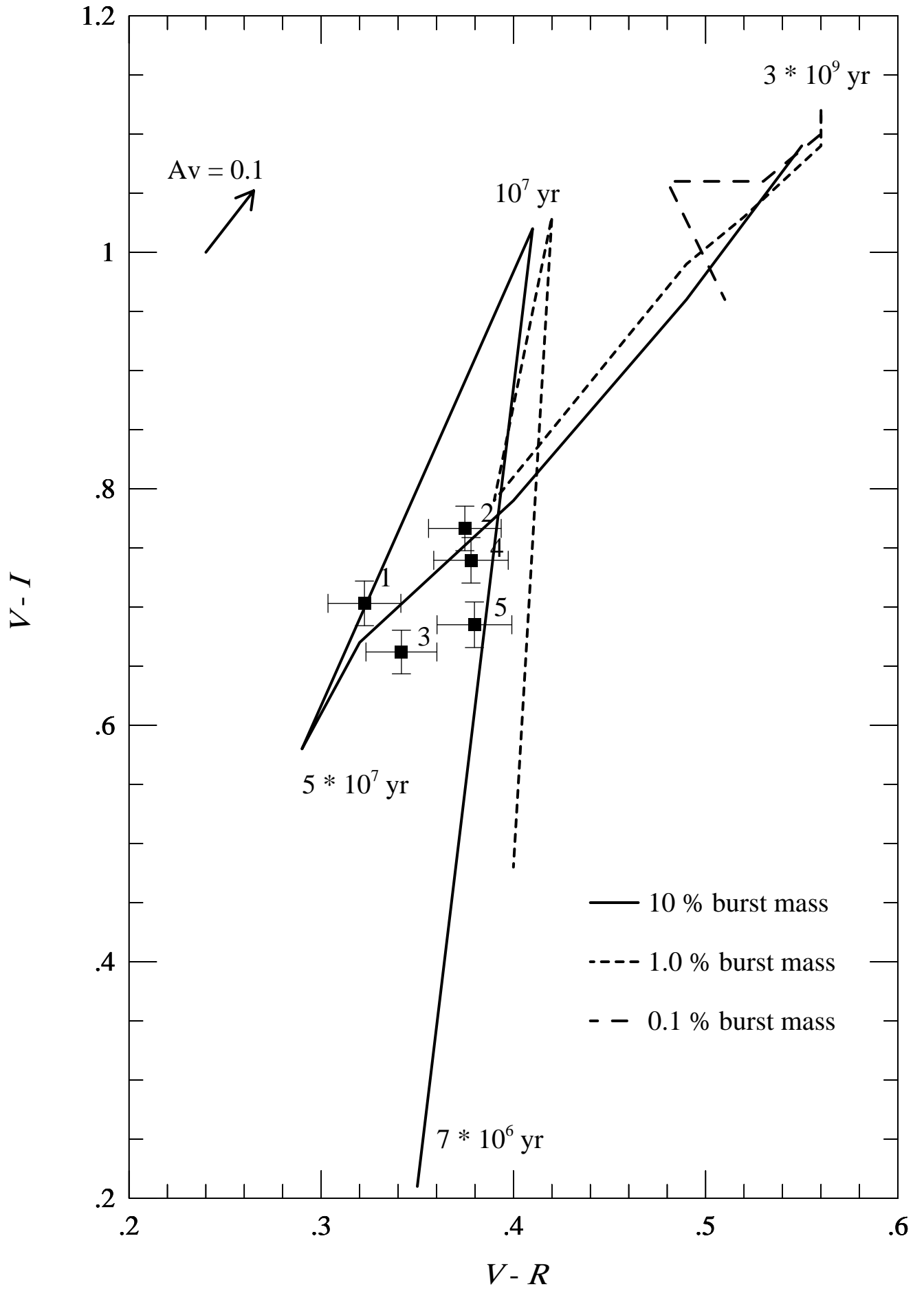
KUG 1016+467



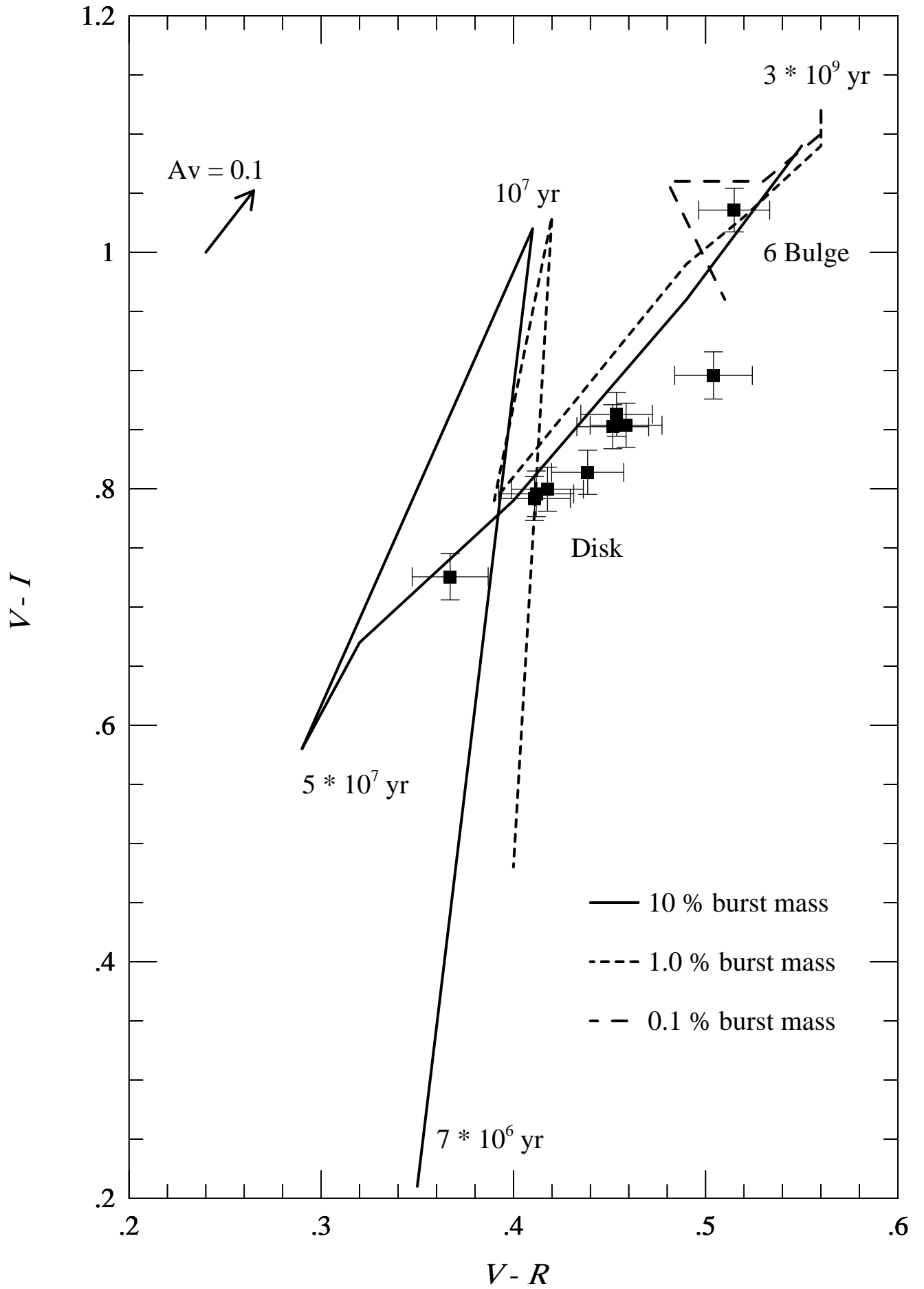
KUG 0908+451



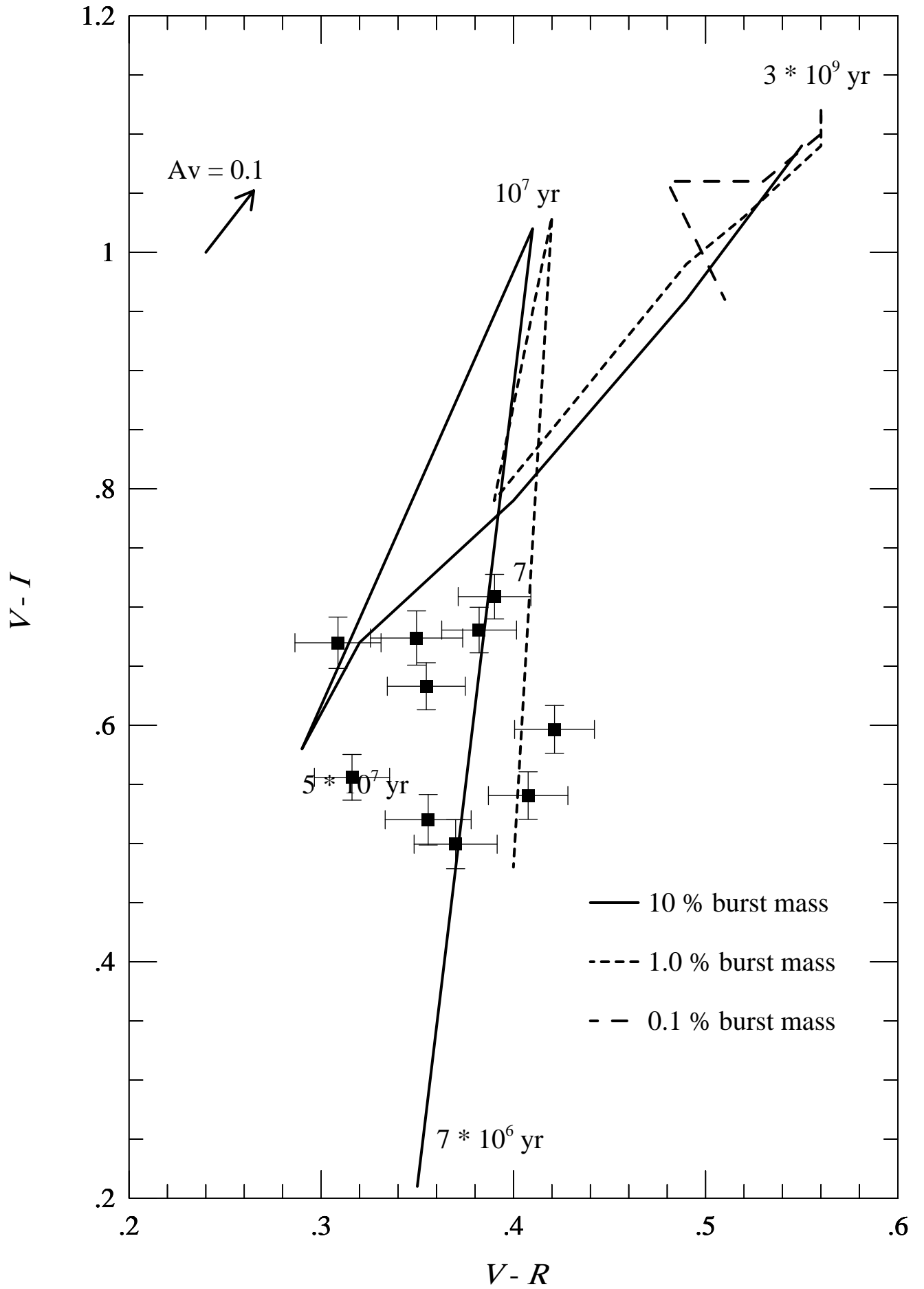
KUG 0908+468



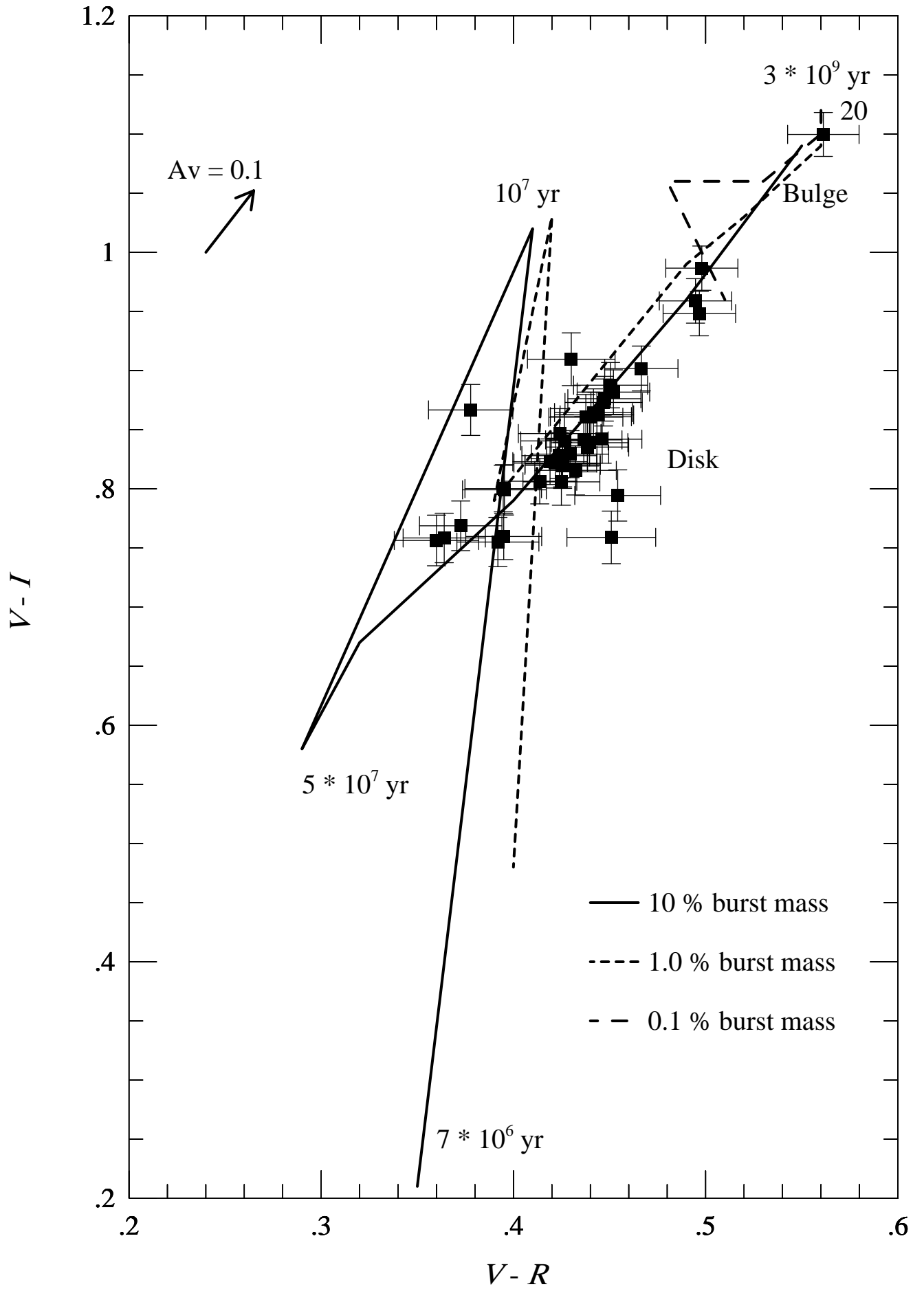
KUG 0911+471



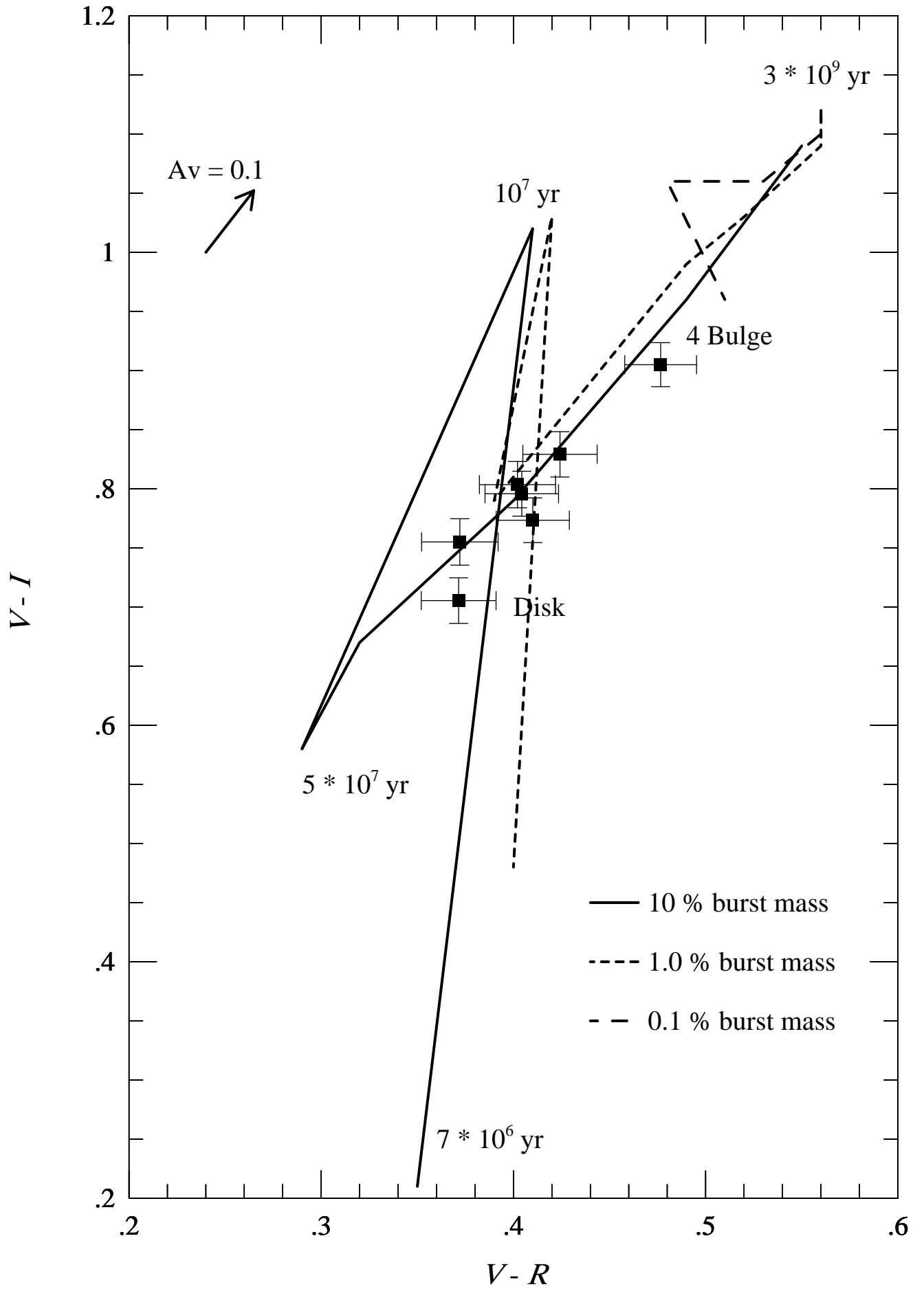
KUG 0919+474



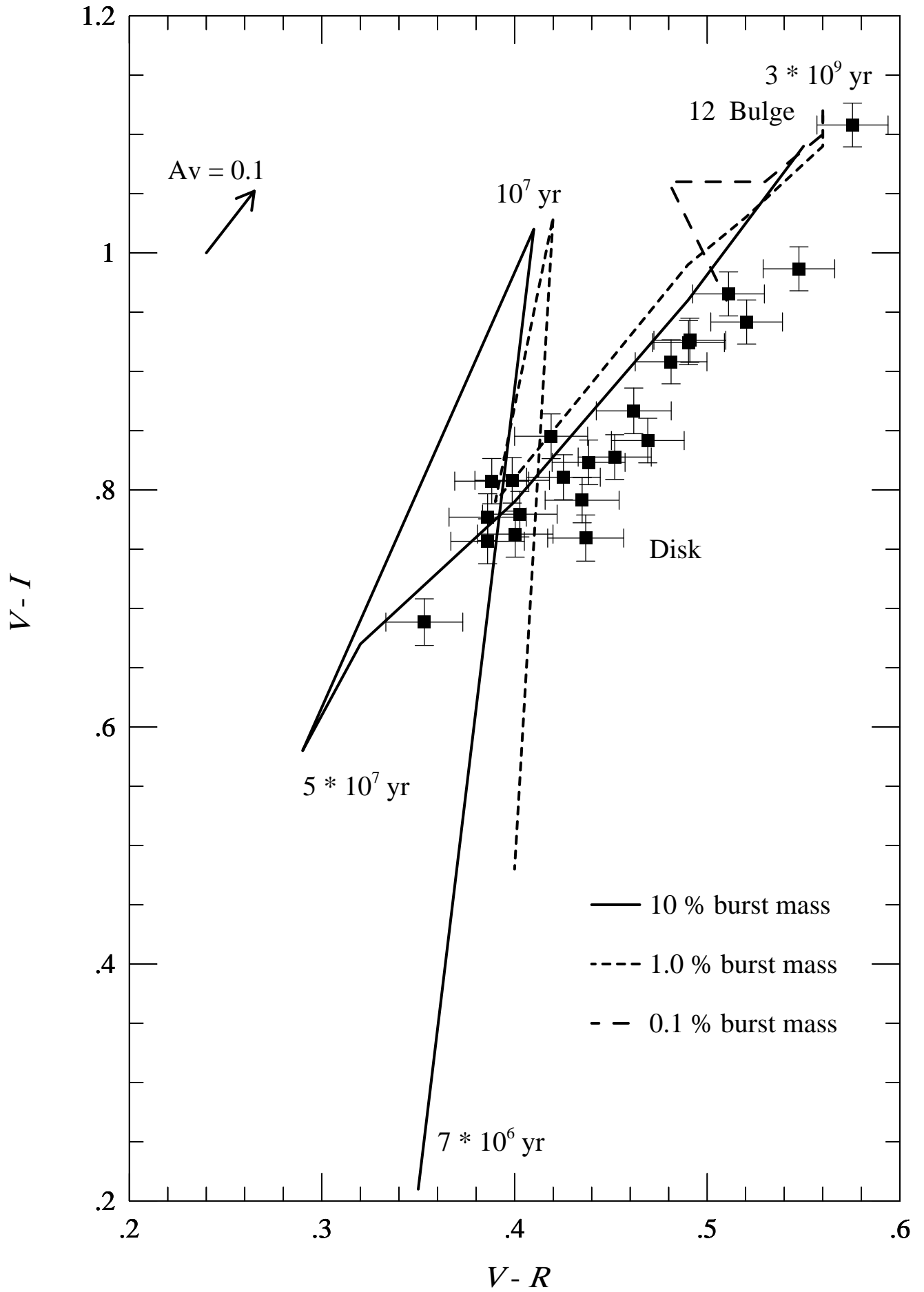
KUG 0924+448



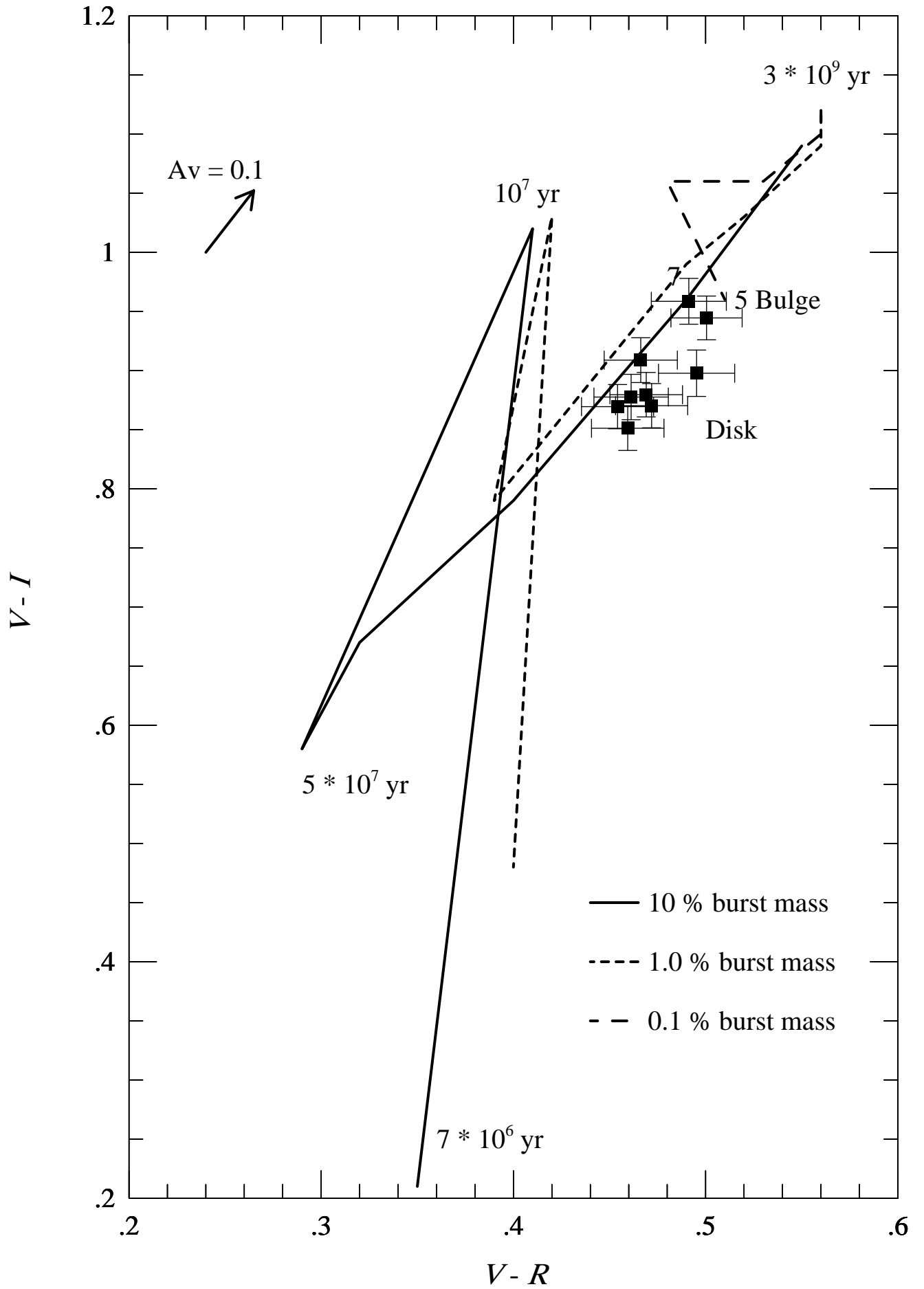
KUG 0944+468



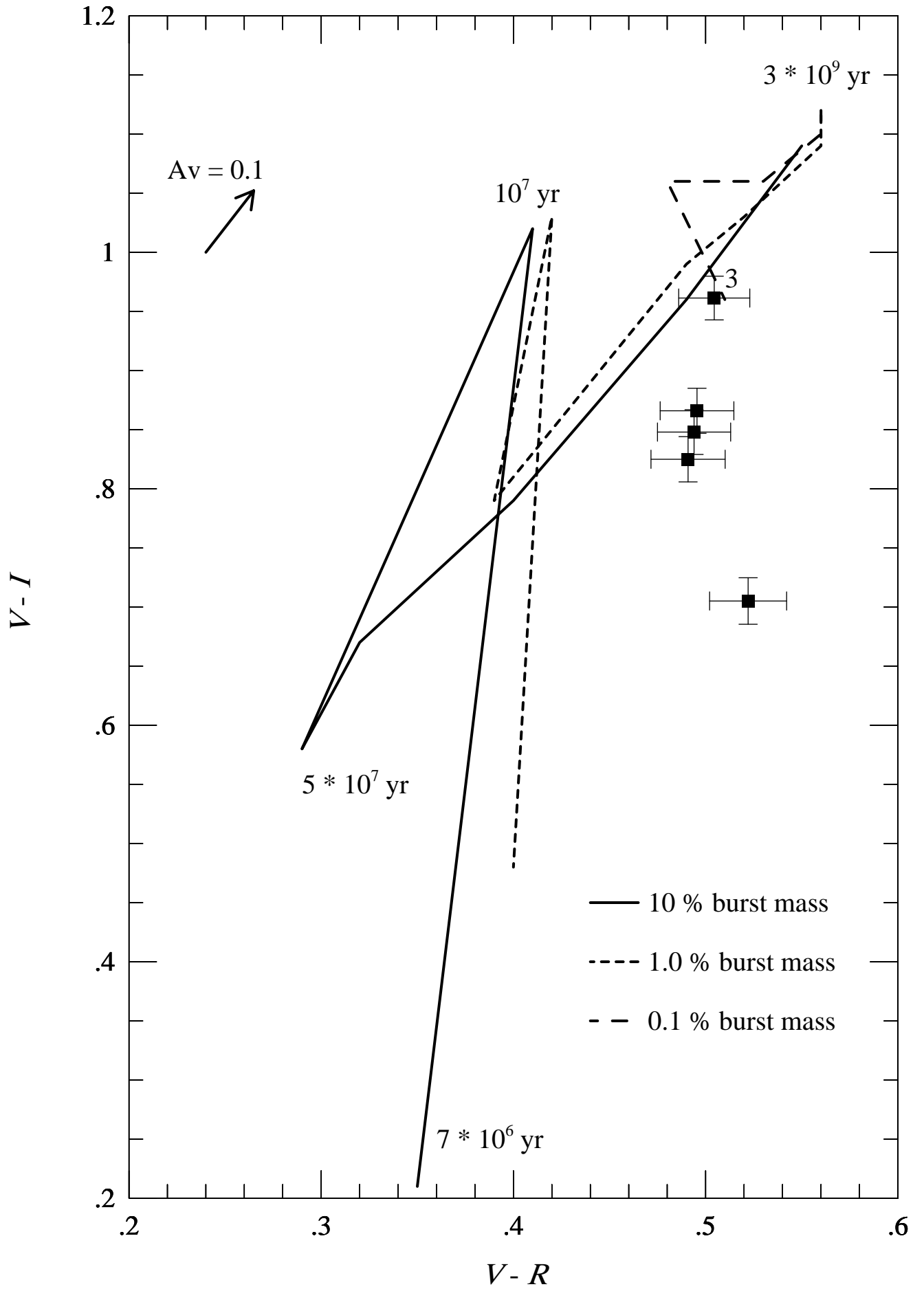
KUG 0945+443



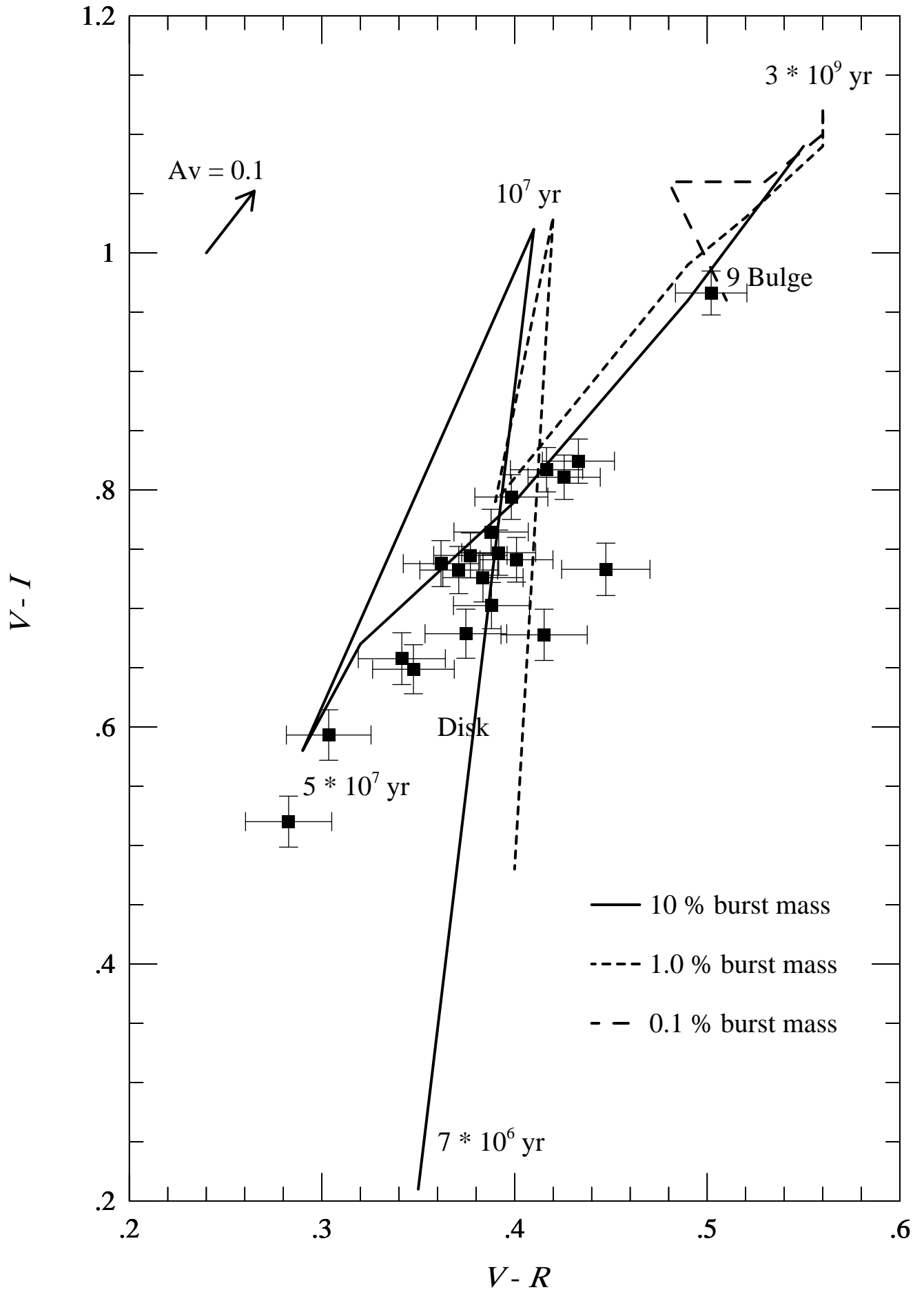
KUG 0947+445A



KUG 0953+466



KUG 1007+461



KUG 1016+467

